Published in final edited form as:
ACS Chem Neurosci. 2011 August 17; 2(8): 411–432. doi:10.1021/cn2000266.

Recent advances in the design and development of novel negative allosteric modulators of $mGlu_5$

Kyle A. Emmitte
Department of Pharmacology, Vanderbilt Center for Neuroscience Drug Discovery, and Department of Chemistry, Vanderbilt University Medical Center, Nashville, TN 37232 USA

Abstract

Negative allosteric modulators (NAMs) of metabotropic glutamate receptor subtype 5 ($mGlu_5$) have remained attractive to researchers as potential therapies for a number of central nervous system related diseases, including anxiety, pain, gastroesophageal reflux disease (GERD), addiction, Parkinson's disease (PD), and fragile X syndrome (FXS). In addition to the many publications with supportive preclinical data with key tool molecules, recent positive reports from the clinic have bolstered the confidence in this approach. During the two year time span from 2009 through 2010, a number of new $mGlu_5$ NAM chemotypes have been disclosed and discussed in the primary and patent literature. A summary of several efforts representing many diverse chemotypes are presented here, along with a discussion of representative structure activity relationships (SAR) and synthetic approaches to the templates where possible.

Keywords

metabotropic glutamate receptor 5; negative allosteric modulator; anxiety; pain; gastroesophageal reflux disease; addiction; Parkinson's disease; fragile X syndrome

Introduction

Glutamate (L-glutamic acid), the major excitatory transmitter in the mammalian central nervous system (CNS), exerts its effects through both ionotropic and metabotropic glutamate receptors thereby generating the fast excitatory synaptic responses at the majority of CNS synapses. While ionotropic glutamate receptors are ligand-gated ion channels responsible for mediation of glutamate fast transmission, the metabotropic glutamate receptors (mGlus) belong to family C of the G-protein-coupled receptors (GPCRs) and modulate the strength of synaptic transmission. The mGlus are characterized by a seven transmembrane (7TM) α-helical domain connected via a cysteine rich-region to a large bi-lobed extracellular amino-terminal domain. While the orthosteric binding site is contained in the amino-terminal domain, currently known allosteric binding sites reside in the 7TM domain. The eight mGlus discovered to date have been divided according to their structure, preferred signal transduction mechanisms and pharmacology (group I: $mGlu_1$ and $mGlu_5$; group II: $mGlu_2$ and $mGlu_3$; group III: $mGlu_4$, $mGlu_6$, $mGlu_7$, and $mGlu_8$). Group I mGlus are located post-synaptically and are coupled via G_q to the activation of phospholipase C, which leads to the elevation of intracellular calcium (Ca^{2+}) and activation of protein kinase

Corresponding Author: Kyle A. Emmitte, Department of Pharmacology, Vanderbilt Center for Neuroscience Drug Discovery, Vanderbilt University Medical Center, Nashville, TN 37232-6600, USA. kyle.a.emmitte@vanderbilt.edu; Phone: 615-936-8401; Fax: 615-343-6532..
Author Contributions K.A.E. researched the patent and primary literature, wrote the manuscript, and prepared all figures, schemes, and tables.

C (PKC). Both group II and group III mGlus are located pre-synaptically and are coupled via G_i/G_o to the inhibition of adenylyl cylase activity.[1,2]

The mGlus have long been considered attractive therapeutic targets for a variety of neurological and psychiatric disorders. As such, several small molecule mGlu agonists and antagonists that compete with glutamate for the orthosteric binding site have been developed and studied.[3] Still, selectively targeting a specific mGlu through the use of an orthosteric ligand has proven difficult due to the highly conserved nature of that binding site. Furthermore, many orthosteric agents are glutamate derivatives or analogues of glutamate and thus lack the pharmacokinetic or CNS penetration properties desirable in a small molecule probe. A strategy that has proven more effective for achieving selectivity has been the design and use of allosteric modulators of the target. Allosteric modulators that do not activate the receptor directly but instead potentiate the activation induced by glutamate are known as positive allosteric modulators (PAMs). Conversely, molecules that bind to an allosteric site and act as noncompetitive antagonists are termed negative allosteric modulators (NAMs). In addition to the aforementioned selectivity advantages, the location of known allosteric binding sites in the transmembrane domain of the receptor has allowed for the synthesis of molecules with the balance of physiochemical properties required for penetration of the CNS.[4,5,6]

The study of $mGlu_5$ and its relation to disease has been aided tremendously by the identification and characterization of two related tool compounds that function as noncompetitive antagonists of that receptor. These molecules are the simple 1,2-diarylalkynes 2-methyl-6-(phenylethynyl) pyridine (MPEP)[7] and 3-[(2-methyl-1,3-thiazol-4-yl)ethynyl]pyridine (MTEP)[8] (Figure 1). These important tool compounds have exhibited efficacy in numerous preclinical models of disease, including pain,[9] anxiety,[10,11,12,13,14] gastroesophageal reflux disease (GERD),[15,16] and fragile X syndrome (FXS).[17,18] In addition, substantial work with these compounds using numerous animal models has furthered the understanding of the link between $mGlu_5$ and drug addiction. These compounds have demonstrated an ability to attenuate various cocaine seeking behaviors in mice,[19,20] rats,[21,22,23,24,25,26] and squirrel monkeys.[27,28] Further work established their efficacy in animal models with other drugs of abuse, including nicotine,[26,29] morphine,[30] methamphetamine,[31] and alcohol.[32,33,34,35,36] Finally, both MPEP and MTEP were recently found to have an antidyskinetic effect in cynomolgus monkeys treated with 4-phenyl-1,2,3,6-tetrahydropyridine (MPTP), a compound that causes rapid onset of Parkinsonism.[37] Such results indicate that antagonism of $mGlu_5$ might constitute an effective therapy for Parkinson's disease levodopa-induced dyskinesia (PD-LID), which is a complication that arises following dopamine-replacement therapy. The body of work surrounding the preclinical *in vivo* characterization of MPEP and MTEP is substantial and bolsters the promise of small molecule antagonists of $mGlu_5$ as therapeutics. As such, research directed toward the discovery of novel $mGlu_5$ NAMs suitable for evaluation in the clinic has been abundant.[38,39,40]

Further indications that a non-competitive antagonist of $mGlu_5$ may translate into an effective therapeutic have been noted in recent years through multiple disclosures from the clinic. Addex Pharmaceuticals has reported positive data from phase II clinical studies with the $mGlu_5$ NAM ADX10059 (general chemical series[41] shown in Figure 1) in both GERD[42] and acute migraine.[43,44] FRAXA Research Foundation and Neuropharm have been exploring the potential of fenobam, a compound discovered and evaluated as an anxiolytic in the 1970s,[45] for treating FXS. In fact, Neuropharm received Orphan Drug Designation for fenobam to treat FXS in 2006. The early results from these studies in patients have been disclosed and were encouraging. Using prepulse inhibition as an outcome measure, 50% of patients (4/6 males and 2/6 females) responded according to the pre-defined criteria of

efficacy.[46] More recent reports from Novartis with their $mGlu_5$ antagonist AFQ056 (general chemical series[47] shown in Figure 1) detailed their efforts directed toward identification of the first approved treatment for PD-LID.[48] The link between $mGlu_5$ antagonism and PD-LID was further bolstered by a recent communication from Addex describing the efficacy of both ADX10059 as well as their second generation $mGlu_5$ antagonist ADX48621 (general chemical series[41] shown in Figure 1) in a non-human primate model of PD-LID.[49,50] While clinical evaluation of ADX48621 continues, further development of ADX10059 was halted in late 2009 due to concerns over elevated alanine transaminase (ALT) levels in Phase IIb studies in GERD patients.[51] Novartis also recently released information from a small trial with AFQ056 in adult FXS patients. Although the trial was insufficient in length to measure effects on basic intelligence and details surrounding the trial have yet to be published, noted improvements in certain aberrant behaviors were reported.[52] AstraZeneca is evaluating two different $mGlu_5$ NAMs, AZD2066 and AZD2516, in multiple clinical studies in a variety of patients, including those who suffer from neuropathic pain and GERD.[53] Phase II studies with Roche's $mGlu_5$ NAM RG7090 in FXS and treatment resistant depression are also ongoing.[54] Seaside Therapeutics recently completed investigational new drug enabling studies with their $mGlu_5$ NAM STX107, which was in-licensed from Merck. Enrollment of a Phase II study of STX107 in FXS patients was slated for 2010.[55] Details related to the chemical structures of the Seaside, Roche, and AstraZeneca compounds are not currently in the public domain.

With so much preclinical and now clinical support for non-competitive antagonism of $mGlu_5$ as a therapeutic approach, activity in this area remains plentiful. Since the advanced compounds where chemical structures are known contain an alkyne functional group, most current efforts are focused on alternative chemotypes. New advancements in this field occur regularly and several recent reviews highlighting progress in the discovery efforts centered on $mGlu_5$ antagonists have been published.[38,39,40] As such, this review will focus on publications of non-alkyne containing series from the primary and patent literature that have occurred during the years 2009 through 2010. In deciding what information to highlight from lengthy patent applications, particular effort was made to include data for those compounds for which *in vivo* data, either pharmacokinetic or behavioral, was disclosed.

AstraZeneca

AstraZeneca published several separate patent applications on the same day (April 30, 2009), disclosing similar 1,2,4-triazole antagonists of $mGlu_5$ (Table 1).[56,57,58] One application highlighted compounds that possessed a chiral ether linkage between the 5-aryl-1,2,4-triazole and a second heterocyclic ring (**1**–**3**).[56] Compounds were characterized in a functional assay that measured their ability to block calcium mobilization in the presence of an agonist in cells expressing human $mGlu_5$. Further information was provided describing the brain to plasma ratio in rats following administration of the compound. The highlighted chiral ether linked compounds were quite potent; however, brain penetration was poor. Another application presented molecules with an amide linkage between the two heteroaryl rings (**4**–**5**).[57] These molecules were less potent; however, brain penetration was improved. Significantly more data was presented in the third application, which focused on alkyl amine linkages (**6**–**11**).[58] Brain penetration remained generally poor with these compounds; however, it could be improved somewhat as evidenced by *N*-methylpyridone **9**. The improvement may have been due to the removal of the hydrogen bond donor in the eastern aromatic ring. Similar brain penetration was observed with a more potent 3-chlorophenyl analogue **10** in the context of an eastern pyrimidine ring, which also lacked a hydrogen bond donor. Also of note is the negative effect on brain penetration observed with the oxadiazole **11** compared to isoxazole **9**. The synthetic route for isoxazole **10** (Scheme 1) is representative of the series (yields shown where provided).[58,59] Theroute began with 3-

chloroacetophenone **12**, which was reacted with sodium hydride and subsequently diethyl oxalate to afford dioxobutanoate **13**. Conversion to isoxazole **14** was accomplished through treatment with hydroxylamine hydrochloride. Reduction of the ester functionality was performed with lithium aluminum hydride to give alcohol **15**, which was subsequently converted to mesylate **16** using standard conditions. Reaction with the sodium anion of aminotriazole **17** gave the final compound **10**. The intermediate **17** was prepared in low yield via a single step through the reaction of acid chloride **18** with aminoguanidine **19**. Such a route is readily amenable to rapid variation of the eastern aromatic ring portion of the chemotype.

An additional six applications were filed on the aforementioned date and described a concept based on the incorporation of a conformational restraint into the previously described alkyl amine linked analogues (Figure 2).[60,61,62,63,64,65] The concept involved a carbon-carbon bond formation between the *N*-alkyl group at the 3-position of the 1,2,4-triazole and the methlyene linker on the isoxazole, thus generating a cyclic tertiary amine. As before, potency and rat brain penetration data was disclosed for selected compounds in each application. The majority of the compounds for which such data was presented contained an isoxazole ring bound to the cyclic amine (Table 2). In the context of a pyrrolidine constraint with an *R*-configuration at the lone stereocenter, potent analogues were seen with carboxamide **20**[62] and aminopyridine **21**.[63] Both compounds also demonstrated low rat brain to plasma ratios; however, analogous to the prior series, brain penetration could be improved by removal of the hydrogen bond donors on the eastern ring as evidenced by dimethylaminopyridine **22**.[63] Although, the dimethylation of **21** improved the brain to plasma ratio by over three-fold, it also resulted in more than a ten-fold decrease in potency. One application focused on thiophene replacements for the western phenyl ring of the template (**23–25**).[64] Also contained in this application were some 2-azabicyclo[3.1.0] derivatives such as **24**. Such a modification to the pyrrolidine core appears to have little effect on potency while demonstrating some improvement in brain penetration (compare **24** to **23**). Again, the compound with the highest brain to plasma ratio (**25**) lacked a hydrogen bond donor. The remaining application provided additional 2-azabicyclo[3.1.0] examples (**26–27**) as well as 3-azabicyclo[3.1.0] analogues such as **28**.[65] Potency remains similar across these examples, but brain to plasma ratios were not reported for any of the 3-azabicyclo[3.1.0] derivatives. Of note is the fact that 2-chlorothiophene **24** demonstrated higher brain to plasma ratio than its 3-chlorophenyl direct comparator **26** without compromising potency. Although specific yields are not reported for most steps, the synthesis of **22** (Scheme 2) is representative for these analogues.[63] The sequence began with the chiral pyrrolidine-2-carbaldehyde **29** which was subjected to a one-pot, three step procedure[66] to afford isoxazole **30**. Removal of the *t*-butyl carbamate protecting group was accomplished upon treatment with trifluoroacetic acid, and the resultant amine was reacted with methyl isothiocyanate to provide thiourea **31**. Treatment with sodium *tert*-butoxide and methyl iodide gave methylated product **32**, which was subsequently reacted with hydrazide **33** in a microwave assisted process to provide final compound **22** in low yield.

Nearly a year after the simultaneous disclosure of these series, another application describing a series of related sulfide bridged analogues was published (Table 3).[67] The selected compounds within this application where $mGlu_5$ functional activity and rat brain to plasma ratios were reported were closely related chiral analogues having a methyl group (*R* configuration) appended to the carbon bridging the western heteroaryl ring to the sulfur atom. In cases where the eastern ring was a pyridone, the activities of the tetrazole and oxadiazole analogues were similar (compare **34** to **37** and **35** to **38**); however, the corresponding isoxazoles **40** and **41** are noticeably less potent. Interestingly, modification of the eastern ring to a pyridazinone restores the loss in potency (compare **42** to **36** and **39**). Most of these analogues demonstrated very low brain to plasma ratios; however, as was seen

previously, removal of the hydrogen bond donor improved brain penetration in certain cases (compare **35** to **34** and **38** to **37**). The synthetic route for isoxazole **42** (Scheme 3) is representative of the series. The synthetic sequence began with ester **43**, and reaction with methyl Grignard afforded the methyl ketone **44**. An enantioselective borane reduction using a chiral oxazaborolidine catalyst[68] was used to provide the chiral secondary alcohol **45**. Mesylate **46** was prepared using standard methods and reacted with thione **47** under basic conditions to afford final compound **42**. Thione **47** was prepared from the reaction of carbohydrazide **48** with isothiocyanatomethane.

Gedeon Richter

Work from Gedeon Richter recently described a hit to lead effort in 1,2,4-oxadiazole and tetrazole series that were structurally related to the AstraZeneca compounds outlined above.[69] High throughput screening (HTS) of their internal compound collection led to the identification of oxadiazole hit **49** as an $mGlu_5$ NAM with modest potency (Figure 3). Two different *in vitro* assays were used to characterize compounds. The first assay ($mGlu_5$ K_i) was a cell based binding assay that measured affinity of the compound for the MPEP binding site using the radioligand [^{3}H]-2-((3-methoxyphenyl)ethynyl)-6-methylpyridine (M-MPEP), a derivative of MPEP.[70] The second assay was a functional cell based assay that measured the ability of the compound to block calcium mobilization in the presence of the orthosteric agonist (*S*)-3,5-dihydroxyphenylglycine. As another means of assessing the quality of compounds generated in the hit to lead process, both size independent ligand efficiency (SILE)[71] and lipophilic ligand efficiency metrics (LELP)[72] were monitored. LELP was introduced by this group as a measure of the price of ligand efficiency paid in logP. As such, higher LELP values are indicative of less drug-like compounds. Evaluation of this scaffold was conducted in three separate areas of the chemotype: phenyl ring substituent(s), cyclic amine, and the amide.

Parallel synthesis was used to prepare over 650 oxadiazole analogues and over 600 tetrazole analogues that met criteria (>85% purity by LC-MS) for testing. The 2-piperidinyl, 2-pyrrolidinyl, and 4-thiazolidinyl derivatives were found most active, while 3-piperidinyl analogues were less potent. Selected compounds from these efforts are depicted here (Table 4). In the oxadiazole series, functional activity can be improved by modification of the aryl substituent as evidenced by the enhanced potency of 3-methylphenyl analogue **50** and 3-methoxyphenyl analogue **51** relative to hit compound **49**. The 2-pyrrolidine derivatives **52** and **53** were both similar in binding affinity to the 2-piperidine compounds; however, these compounds were significantly weaker in the functional assay. 4-Thiazolidine analogue **54** does not exhibit a similar discrepancy between the two assays. The tetrazole compounds demonstrated enhanced potency and binding affinity relative to their oxadiazole counterparts (compare **55** to **49** and **56** to **50**). While all of the oxadiazole compounds were prepared and tested as racemates, tetrazole **55** was prepared as its individual pure enantiomers. Testing revealed that (*R*)-**55** ($mGlu_5$ K_i = 58 nM) displayed enhanced binding affinity relative to (*S*)-**55** ($mGlu_5$ K_i = 741 nM). The authors point out that this trend of preference for the (*R*)-enantiomer held up across multiple analogues. Interestingly, the 2-piperidine to 2-pyrrolidine modification does not result in the same dramatic discrepancy between the functional potency and binding affinity seen with the oxadiazoles (compare **58** to **53**). Analysis of their efficiency metrics led the authors to conclude that **56** represented an improved lead relative to the original hit **49**. The synthetic route employed to access tetrazole analogues such as these is shown here (Scheme 4) in the context of the 2-piperidyl amides. The route began by conversion of Boc-protected piperidine-2-carboxylic acid **59** into its corresponding Weinreb's amide. Subsequent treatment with lithium aluminum hydride afforded aldehyde **60**, which was reacted with tosylhydrazide to give hydrazone **61**. Commercially available anilines **62** were converted into their corresponding diazonium salts

63 and then reacted with hydrazone **61** to provide the tetrazoles **64**. Deprotection under acidic conditions gave the free amines, which were coupled with various commercially available carboxylic acids in a parallel synthesis paradigm to yield the final products **55–57**. The incorporation of the substituted phenyl rings at a late stage and the acid monomers in the final step makes the route particularly amenable to the parallel synthesis approach employed in this endeavor.

Another series of $mGlu_5$ NAMs emerged from the HTS screen of the Gedeon Richter compound collection and was also described recently.[73] The carbamoyloxime hit **65** demonstrated an affinity for the known MPEP binding site and behaved as a noncompetitive antagonist in the functional cell-based assay (Figure 4). Following resynthesis of **65** and separation of the *E* and *Z* isomers, it was established that the *E* isomer **66** was the more active compound. An SAR plan was implemented that centered on four separate portions of the template, which were identification of replacements for the imidazole ring, potential alternatives to the cyclohexane ring, optimization of the linker between the cyclohexane ring and aniline, and substitution of the aniline ring. Tolerance for these modifications was limited with the linker and cycloalkyl ring, and most active compounds maintained the carbamoyl oxime linked to the cyclohexane. Substitution of the aniline ring with small substituents such as chloro at the *meta*-position improved affinity and enhanced activity. The majority of SAR was developed through exploring potential replacements for the imidazole ring and selected examples are described here (Table 5). Introduction of the 3-chloro substituent onto the aniline in the context of the imidazole ring provided **67**, which demonstrated enhanced activity relative to **66**. Compound **67** was separated into its individual enantiomers by preparative HPLC, and it was determined that the activity of **67** resulted primarily from a single enantiomer ((+)-**67** $mGlu_5$ K_i = 8.8 nM; (−)-**67** $mGlu_5$ K_i > 1000 nM). Compound **67** was examined in the Vogel punished drinking test[74] in rats and demonstrated significant efficacy at doses as low as 5 mg/kg using intraperitoneal (IP) dosing. Several replacements were tolerated in place of the imidazole ring and provided analogues with similar activity to **67**. Examples include 2-thiophenyl analogue **68**, phenyl analogue **73**, and 3-fluorophenyl analogue **74**. On the other hand, the 3-thiophenyl analogue **69** had reduced activity relative to **67** while the saturated 4-morpholinyl analogue **70** had no demonstrated affinity in the binding assay. Enhanced activity was observed with 2-pyridyl analogue **71** and 3-pyridyl analogue **72**. In fact, **72** was the most potent compound in the functional assay disclosed in this manuscript. Several active analogues were also tested for their ability to functionally inhibit $mGlu_1$ and $mGlu_2$ and demonstrated good selectivity for $mGlu_5$. The synthesis of **67** is representative of the series and shown here (Scheme 5). Readily prepared ketone **75** was reacted with hydroxylamine to generate the oxime. The *E* and *Z* isomers were separated either by crystallization or chromatography to afford the pure *E* isomer **76**. Treatment with isocyanate **77** provided the final compound **67**.

GlaxoSmithKline

A novel thiazolotriazole mGlu5 NAM chemotype was discovered through a HTS of the GlaxoSmithKline compound collection.[75] With relatively low molecular weight, high polarity, ligand efficiency, and selectivity over other mGlus, the chemotype was deemed worth further exploration. A synthetic route was employed (Scheme 6) that allowed for variation of four distinct portions of the scaffold. Substituted 1,2,4-triazolethiones **78** were reacted with haloketones **79** to provide 5-carbonyl substituted thiazolotriazoles **80**. Reduction of the carbonyl group was accomplished upon treatment with sodium borohydride to afford alcohols **81**. Conversion to the carbamate final compounds **82–91** was accomplished by reaction either with the appropriate isocyanates or with carbonyl diimidazole and the appropriate primary amines. SAR developed within this template using a cell-based calcium mobilization assay revealed that $mGlu_5$ activity was sensitive to small

structural modifications (Table 6). For instance, while neither the 6-methyl group on the thiazole (**83**) nor the methyl group on the sp^3 carbon bridging the heterocycle and carbamate (**84**) provide much improvement relative to unsubstituted analogue **82**, the combination of both substituents provided potent analogue **85**. Hypothesizing that free brain concentration would be critical to achieving occupancy in vivo, the fraction unbound (f_{ub}) in rat brain homogenates was monitored for key compounds.[76] Researchers sought to balance functional potency with free brain concentration by maximizing a parameter termed $pIC_{50}eff$ (pIC_{50} + log10[f_{ub}]). While saturation of the aniline ring in the form of cyclohexyl analogue **86** resulted in a loss of potency, substitution at the meta-position of the aniline ring with either chloro (**87**) or fluoro (**88**) improved potency slightly. Unfortunately the fraction unbound was considerably reduced with **87** and **88** relative to **85** resulting in a lower $pIC_{50}eff$ value. Conversely, pyridyl analogue **89**, while less potent than **85**, had a similar $pIC_{50}eff$ value due to its larger fraction unbound. Substitution at the 2-position of the thiazolotriazole with cyclopropyl (**90**) or aryl groups such as thiophene (**91**) also improved potency. Fraction unbound with **91** was the lowest reported, making the compound less interesting for further studies. The noncompetitive nature of **85** was verified through in vitro studies, and it was also shown to bind to the known MPEP binding site using [^{3}H]-MPEP. Separation of **85** into its respective enantiomers by HPLC revealed a pronounced preference for a single enantiomer ((*R*)-**85** $mGlu_5$ IC50 = 40 nM; (*S*)-**85** $mGlu_5$ IC_{50} > 10,000 nM). Evaluation of (*R*)-**85** in a rat pharmacokinetic study demonstrated that the compound was both bioavailable and CNS penetrant (F = 28%; AUC brain:blood = 2.0). Finally, evaluation of (*R*)-**85** in the mouse marble burying model of anxiety established its efficacy at a dose as low as 5 mg/kg when dosed orally.[77]

Eli Lilly

A relatively narrow patent application from Eli Lilly recently described a series of isothiazole $mGlu_5$ NAMs.[78] Variation in this template focused on either hydrogen or small alkyl substituents on the cyclopropyl ring (R^1) and indazole nitrogen (R^3) (Figure 5). Claimed substituents at the 6-position of the pyridine (R^2) were broader, but exemplified compounds were generally small alkyl, cycloalkyl, alkylamino, and alkoxy substituents. Synthesis of a key exemplar compound **100** is outlined here (Scheme 7). The route was initiated with a two step kilogram scale synthesis of aminoisothiazole **93** from thioamide **92**. Reaction of **93** with acid chloride **94** provided amide **95**. Treatment of **95** with bromine and aqueous sodium hydroxide induced a deacylation/bromination reaction to afford **96**. The Suzuki coupling of **96** with the custom prepared boron reagent **97** gave intermediate **98**, which was reacted with arylstannane **99** in a Stille coupling to afford the final compound **100** (yield not provided). Compounds exemplified in this patent were tested in a functional calcium mobilization assay and found to have IC_{50} values less than 75 nM. Analogue **100** was determined to have an IC_{50} equal to 9.5 nM. The hydrochloride salt of **100** was examined in a stress-induced hyperthermia (SIH) rat model, which is a well known model of anxiety.[79] Rats were dosed orally at 0.3, 1.0, 3.0, and 10 mg/kg and immediately placed in their home cage in a dark room. After the 60 minute pretreatment, the animals were individually relocated to a brightly lit room and the first core body temperature (T1) was determined. The second core body temperature reading (T2) was made ten minutes later. The difference between T2 and T1 constituted the SIH response. Compound **100** produced a 35% reduction in the SIH response relative to vehicle at a dose of 3.0 mg/kg.

Lundbeck

A patent application from Lundbeck was recently published describing a series of adamantyl diamides.[80] The application contains over 250 exemplified compounds from this general series. Preparation of symmetrical diamides was readily accomplished through coupling of

adamantine-1,3-diamine **101** with suitable carboxylic acids or acid chlorides (Scheme 8). For example, a standard coupling reaction with acid **102** afforded diamide **103**, and reaction with acid chloride **104** provided diamide **105**. In the case of unsymmetrical diamides, several different synthetic routes were employed. In an example of one method, adamantine-1,3-diamine **106** was first converted to amide **107** in low yield and subsequently reacted with acid chloride **108** to afford diamide **109** (yield not provided) (Scheme 9). A longer, more scalable route with higher yields was exemplified by the synthesis of analogue **116** (Scheme 10). The route began with 1-adamantanecarboxylic acid **110**, which was transformed via a Ritter reaction to acetamide **111**. Cleavage of the acetamide with concentrated hydrochloric acid was followed by conversion of the intermediate to methyl ester **112**. Reaction with acid chloride **104** afforded amide **113**. Hydrolysis of the methyl ester followed by a Curtius rearrangement gave amine **114**, which was then coupled with carboxylic acid **115** to yield diamide **116**. Related analogues **117** and **118** were also prepared via the same route.

Although, compounds in the application were characterized in both a radioligand binding assay using [^{3}H]-3-methoxy-5-(pyridin-2-ylethynyl)pyridine (mPEPy),[81] a close structural analogue of MPEP, as well as a calcium mobilization assay in HEK293 cells that expressed rat $mGlu_5$, data provided for specific compounds was limited. Binding affinity values were reported for analogues **103** ($mGlu_5$ K_i = 6.7 nM) and **105** ($mGlu_5$ K_i = 40 nM). While the lack of specific in vitro data makes determination of SAR difficult, of particular interest was the reported in vivo activity of selected compounds (Table 7). Compounds were evaluated for their anxiolytic effects in a mouse marble burying model[77] as well as a modified Geller-Seifter conflict test in rats.[82] While the mouse studies were conducted with subcutaneous dosing, the rat studies used oral dosing. Without functional activity and exposure data, it is not possible to draw correlations to the efficacy data; however, several compounds demonstrated efficacy in the 10 to 30 mg/kg dose range.

Merz

A recent patent application from Merz contained over 300 exemplified compounds from a 6-halopyrazolo[1,5-*a*]pyrimidine series.[83] Although biological data was not provided for the majority of these compounds, selected compounds were characterized in two cell-based functional assays as well as a radioligand binding assay with [^{3}H]-M-MPEP (Table 8). Both functional assays were calcium mobilization assays that measured the compounds ability to potentiate the response to the orthosteric agonist L-quisqualic acid. One functional assay was run in stably transfected Chinese hamster ovary (CHO-K1) cells that express human $mGlu_5$, while the second was run in primary astrocytes prepared from cortices of newborn rats. In general, there was good agreement between the three assays, and the SAR trends were similar. tetrahydrocinnoline amides **119** and **120** (Series I) do not contain a chiral center; however, the tetrahydropyrrolopyrazine amides **121**–**126** were substituted with a methyl group at the 1-position of the ring, resulting in a chiral center. Potency and binding affinity of these analogues was enhanced by the replacement of the 6-methyl substituent on the tetrahydropyrrolopyrazine ring with a chloro or bromo substituent (compare **123** and **125** to **121** as well as **124** and **126** to **122**). Also of note is the improved potency observed with the pure enantiomers (*R*)-**122** and (*R*)-**124** relative to their respective racemates. The synthesis of (*R*)-**122** is shown in Scheme **8** and is indicative of the general routes to the pyrazolopyrimidine analogues discussed here. The synthesis of carboxylic acid **130** began with the Fischer esterification and subsequent reduction of nitropyrazole acid **127** to provide aminopyrazole **128**.[84] Treatment of **128** with concentrated hydrochloric acid in the presence of 2-bromomalonaldehyde afforded pyrazolopyrimidine **129**. Hydrolysis of the methyl ester under acidic conditions gave carboxylic acid **130**, which was coupled with amine **131** under standard conditions to provide final compound (*R*)-**122** (yield not provided). The synthesis

of chiral amine **131** was accomplished in two steps beginning with the acid mediated reaction of ethylenediamine with furan **132** to yield pyrrolopyrazine **133**. Asymmetric transfer hydrogenation of **133** with chiral ruthenium catalyst **134** gave **131** in near quantitative yield.

National Institute on Drug Abuse

A group of researchers at NIDA has previously reported on a rational design strategy in an aryl amide series of $mGlu_5$ NAMs.[85,86] Further information regarding continued effort within this general chemotype and additional characterization of selected molecules has been published recently.[87] The synthesis of many of the compounds in this manuscript began with 6-methyl-2-aminopyridine **135** (Scheme 12). Coupling of **135** with aryl carboxylic acids or acid chlorides afforded amides **136–140**. In cases where R^1 (**139**) or R^2 (**140**) was a bromide, those analogues were further reacted with aryl boronic acids using Suzuki coupling conditions to generate additional analogues **141–147**. Compounds were characterized in a calcium mobilization assay ($mGlu_5$ IC_{50}) run in HEK293 cells that expressed rat $mGlu_5$ as well as a radioligand binding assay ($mGlu_5$ K_i with [^{3}H]MPEP (Table 9). In general, there was good agreement between these assays; however, there were some exceptions. Prior work in this series had shown that simple exchange of a chloro substituent (**136**) for a cyano group (**137**) produced a near 4-fold improvement in potency.[85] The further introduction of a 5-fluoro substituent to provide analogue **138** further enhanced activity by over 20-fold. Replacement of the cyano group with a 3-pyridyl ring (**141**) was not well tolerated; however, introduction of a phenyl ring at the R^2 position of **137** gave biaryl analogue **142**, which was among the most potent of analogues tested. Interestingly, the cyano group was shown to be essential as analogue **143** demonstrated dramatically reduced affinity in the radioligand binding assay. Fluorinated analogues of **142** (**144–145)** were similarly potent; however, there was a disparity between the binding affinity and functional potency observed with **145** that was not seen with **144**. Replacement of the phenyl group with a 1-naphthyl (**146**) or a 3-pyridyl (**147**) ring was not favorable. Compounds were also evaluated in mGlu subtype functional assays and none demonstrated more than 70% inhibition of phosphatidylinositol (PI) hydrolysis at a concentration of 10 μM. Further, compounds **142** and **144** demonstrated only weak activity in off target assays measuring interactions with the dopamine, serotonin, and norepinephrine transporters.

Concurrent to their work in the aforementioned aryl amides, NIDA reported on similar efforts in several biaryl chemotypes, including 7-substituted quinolines.[88] As the biaryl quinoline template was among the most promising, work was continued in that chemotype and recently disclosed.[89] New 7-phenylquinoline analogues were prepared by the synthetic route shown here (Scheme 13). Bromination of 3-chlorobenzonitrile **148** with 1,3-dibromo-5,5-dimethylhydantoin **149** according to the literature procedure afforded aryl bromide **150**.[90] A Suzuki coupling with boronic acids **151–153** gave the biaryl products **154–156**. A second Suzuki coupling between the aryl chloride and boronate ester **158** was accomplished in the presence of phosphine ligand **157** to afford the final products **159–161**. A modified synthetic approach was used to access 7-(pyridin-3-yl)quinoline (Scheme 14). The route began with either 5-bromonicotinonitrile **162** or 5-bromo-2-chloronicotinonitrile **163**, which was prepared through chlorination of pyridine **161**. Suzuki coupling with boronate ester **158** afforded biaryls **164** and **165**. A second Suzuki coupling of **165** with phenyl boronic acid **151** using phosphine ligand **157** provided analogue **166**. The profile of quinoline analogues in both the functional and radioligand binding assays is shown here (Table 10). Unsubstituted analogue **167** was prepared and reported previously by NIDA,[87] and it was also independently prepared and discussed previously by a group at Pfizer.[91] The addition of phenyl (**151**) or 4-fluorophenyl (**153**) substituents led to compounds with similar binding affinity to **167**; however, potency in the functional assay was reduced significantly.

Introduction of a 3-pyridyl (**152**) group alleviated the discrepancy between the two assays, but both affinity and potency were compromised relative to **167**. Alteration of the scaffold to introduce a pyridyl nitrogen in the internal ring was more successful as both unsubstituted analogue **164** and phenyl substituted analogue **166** were similar in activity to **167**. Intermediate chloropyridine **165** was also tested and although it was weak in both assays, the compound was a clear partial antagonist in the functional assay. In this case, the concentration response curve with **165** reached only a 50 % inhibition of the EC_{80} glutamate response. Subtle SAR between full and partial antagonists has been previously noted within alkyne chemotypes in the literature.[92,93]

Novartis

A HTS based on the ability of compounds to inhibit agonist induced elevation of intracellular calcium (Ca^{2+}) was used by Novartis to identify a novel nicotinamide series of $mGlu_5$ NAMs. A recent publication described a thorough evaluation of the SAR within this chemotype.[94] Two general synthetic routes were used to access compounds within this template (Scheme 15). One route allowed for the introduction of the eastern portion of the chemotype as the final step. Acid chlorides **168** were reacted with amines to yield amides **169**. Subsequent S_NAr reaction with aryl amines **170** under acidic conditions afforded the final compounds **171–183**. A second route used an amide coupling of the hydrolyzed esters of **185** as the final step. The esters **185** were prepared from a Buchwald coupling of aryl amines **170** with 2-chloropyridines **184**. The HTS hit and starting point for SAR development was piperidinyl amide **171** (Table 11). Evaluation of other secondary amine amides indicated that piperidinyl (**171**) and azepanyl (**173**) amides were superior to pyrrolidinyl (**172**) and azocanyl (**174**) amides, and the majority of the remaining SAR was developed in the context of piperidinyl amides. The importance of the 4-chloro substituent on the aniline moiety was illustrated with unsubstituted aniline analogue **175**. Potency could be partially restored with other 4-substituents (**176–178)**, though not to the level seen with **171**. A 3-fold improvement in potency relative to **171** was seen with the introduction of a chloro group at the 3-position of the pyridine core (**180**). A similar 5-fold improvement was observed when comparing **181** to **179**.

Using the 5-amino-2-methylpyridine analogue **181** as a starting point, further derivatization of the piperidinyl ring was made (Table 12). Compounds were also evaluated for their solubility as well as their stability in rat and human liver microsomes. While incorporation of an ethyl group at the 3-position of the piperidinyl ring improved potency with both enantiomers (**182**), metabolic stability was reduced. Also of note was the difference in solubility observed between the two enantiomers. In the case of the 2-ethyl piperidinyl ring, there was a significant difference in potency between the two enantiomers, with a 12-fold preference for the *R*-configuration relative to the *S*-configuration (**183**). Having determined that (*R*)-**183** offered the optimal balance of properties, the compound was studied in a rat pharmacokinetic study. The compound demonstrated moderate clearance (37.2 mL/min/kg) and good bioavailability (54%). Importantly, CNS penetration with (*R*)-**183** was excellent with a brain to plasma ratio around 1.3 to 1. Given such promising data, analogue (*R*)-**183** was studied in three separate rodent behavioral models of anxiety. The SIH model was evaluated in mice,[79,95] and (*R*)-**183** was efficacious at 3 and 10 mg/kg using oral dosing. Further evaluation in rats was conducted using the Vogel conflict test[74,96] and the fear-potentiated startle test (FPS).[97,98] Dose dependent efficacy was observed with oral dosing in both experiments with significance at 10 and 30 mg/kg in the Vogel test and 3, 10, and 30 mg/kg in the FPS test.

Novartis researchers continued further optimization efforts in the (*R*)-**183** series and published results from that effort recently.[99] Metabolite identification studies revealed that

the piperidine moiety of (*R*)-**183** was a major site of oxidative metabolism. As such, medicinal chemistry was focused on the identification of a suitable bioisosteric replacement. Several heterocyclic alternatives were explored including oxadiazoles, triazoles, and isoxazoles and shown to lack suitable activity for further work. Fortunately a 1-alkyl-2-benzimidazolyl group was identified as a promising alternative and SAR exploration was conducted in that area (Table 13). *n*-Propyl analogue **186**, ethyl analogue **187,** and isobutyl compound **189** were similar in activity while the *n*-butyl analogue **188** was less active. The metabolic stability profiles of **186** and **187** were preferable to those for **188** and **189**. Installation of a chloro substituent at each of the positions on the benzimidazole ring (**190–193**) maintained or reduced intrinsic clearance in both rat and human liver microsomes relative to **186,** with the intrinsic clearance of **191** in rat liver microsomes representing the lone exception. The improved potency and encouraging metabolic stability of **193** led to further study of that compound. Radioligand binding assays with [^{3}H]-ABP688[100] showed that **193** demonstrated a high affinity for the known allosteric binding site ($mGlu_5$ K_i = 2.4 nM). Compound **193** was also shown to be selective against other mGlus (IC_{50} > 10 μM for $mGlu_1$, $mGlu_2$, and $mGlu_7$) and ionotropic glutamate receptors. Although the intrinsic clearance in rat liver microsomes for **193** and (*R*)-**183** were nearly identical, the in vivo profile for **193** was superior. Clearance was lower (15 mL/min/kg), and bioavailability remained good (41%). Furthermore, CNS penetration remained excellent with a brain to plasma ratio around 1.7 to 1. Evaluation of **193** in the FPS model[97,98] using oral dosing demonstrated efficacy in a dose dependent manner with significant responses at both 1 and 3 mg/kg. A four-step synthesis of **193** was employed (Scheme 16). A palladium catalyzed coupling of 2,3-dichloropyridine **194** with amine **195** gave ester **196**, which was hydrolyzed to afford acid **197**. Reaction with 1,2-phenylenediamine **198** in hot polyphosphoric acid (PPA) yielded benzimidazole. Alkylation with *n*-propyl iodide gave the final compound **193** in low yield following separation from its regioisomer **190**.

Sepracor

A rational design approach to new $mGlu_5$ NAMs was employed by researchers at Sepracor, and results from that effort were recently disclosed.[101] Their approach centered on novel methods for tethering two aryl groups as alternatives to traditional linkers such as alkynes, amides, and azoles. Several potential scaffolds were prepared before settling on oxazolopiperidine **200**. Compound **200** was a moderately potent $mGlu_5$ NAM in their functional assay, which was run in an inducible cell line expressing human $mGlu_5$. SAR exploration established the 2-pyridyl ring as optimal for the western portion of the template, and the 3-cyanophenyl ring was similarly optimal for the eastern portion. Additional SAR was established in the interior of the scaffold in the context of these substituents (Table 14). Maintaining the oxazolopiperidine core of **200** in the context of the optimized peripheral groups gave analogue **201**, which was a potent antagonist. The isomeric oxazole **202** was less potent than **201**. The installation of a 5-fluoro group on the phenyl ring boosted potency in both instances (**203** and **204**). Imidazole **205** and thiazole **206** were weak antagonists. While imidazole **207** and triazole **208** were also potent, both were inferior to oxazole **203**. A final modification that further enhanced potency was enlargement of the saturated ring by one carbon to afford azepines **209** and **210**. Radioligand binding assays with **203** and **210** using [$_3$H]-MPEP confirmed their interaction with the known allosteric binding site. Both molecules were also examined for off target activity and were found to have quite clean profiles. With a good correlation between the binding and functional assays, both molecules were examined in occupancy studies in rats using [^{3}H]-mPEPy (Table 15). Compounds were dosed IP and [^{3}H]-mPEPy was dosed by tail-vein injection one hour later. Both compounds showed good CNS penetration; however, **210** was a superior compound, demonstrating an occupancy ED_{50} of 0.9 mg/kg. Compound **210** was next taken into rat and monkey bioavailability studies (Rat: Cl_p = 46.5 mL/min/kg; F = 31%; $t_{1/2}$ = 0.62 h and Monkey: Cl_p

= 16.3 mL/min/kg; F = 10%; t1/2 = 0.67 h). The authors believe such results are less than desirable and plan to continue to work to improve the pharmacokinetics of analogues within this scaffold. The synthesis of **210** is described here (Scheme 17). Piperidinone **211** was brominated to yield bromoketone **212**. Reaction with ethyl diazoacetate in an Eistert homologation afforded azepine **213**. Hydrolysis and decarboxylation was accomplished under acidic conditions. Standard conditions were then used to access azide **214**, which was treated with lithium aluminum hydride to give the amino alcohol **215**. Amide formation through coupling with picolinic acid was followed by a Dess-Martin oxidation to provide ketone **216**. Treatment with Burgess' reagent under microwave conditions gave oxazoloazepine **217**. Removal of the tosyl protecting group, and subsequent Buchwald coupling of amine **218** with 3-bromo-5-fluorobenzonitrile provided the final product **210** in low yield.

Vanderbilt

The Vanderbilt Program in Drug Discovery has used a functional cell-based HTS of a collection of 160,000 compounds to identify 345 confirmed noncompetitive antagonists of $mGlu_5$. The initial report of the SAR within three distinct series that were identified through this screen was reported in early 2009[102] and has been discussed in a prior review.[38] Further efforts with different chemical scaffolds that were discovered through this HTS effort have been communicated since this initial publication. One such effort focused on a series of 6-substituted-4-anilinoquinazolines.[103] Analogues within this series were prepared through reaction of commercially available anilines and the requisite 4-chloroquinazolines using microwave-assisted organic synthesis (MAOS).[104] SAR demonstrated that 4-anilinoquinazolines were superior to the comparator 4-anilinoquinolines and 1-anilinoquinolines, and that the secondary amine was the optimal linker between the quinazoline and the phenyl ring. The majority of SAR evaluation was centered on the 6-position of the quinazoline and on substitution of the aniline ring (Table 16). Potency data for compounds was determined using a functional assay that measured the ability of compound to block the mobilization of calcium by an EC_{80} concentration of glutamate in HEK293 cells expressing rat $mGlu_5$. The screening hit in this series was 6-bromoquinazoline **219**. Substitution of the aniline was critical to potency as evidenced by unsubstituted analogue **220**. Tolerance for substitution was limited although both aryl bromide **222** and methyl analogue **223** were similar in potency to the hit compound. A similar trend was noted with regard to substitution at the 6-position on the quinazoline ring, where chloro (**225** and **229**) and fluoro (**226** and **230**) analogues were also potent antagonists. In this case a 6-nitroquinazoline **227** was also similar in potency to the hit compound. Additional SAR was conducted in context of the 6-fluoroquinazoline (**230–234**), and SAR was somewhat shallow. Analogues **219**, **229**, and **230** were determined to interact with the known allosteric binding site through radioligand binding studies with [^{3}H]-mPEPy. Further, when the same three compounds were tested against other mGlus, all were inactive up to 10 μM, except for $mGlu_1$, where potency was submicromolar in each case.

A third publication from the Vanderbilt group describing the HTS follow up recently appeared.[105] Although the publication describes three distinct chemotypes discovered in the HTS, the majority of the SAR discussion centers on an *N,N'*-(1,3-phenylene)diamide series. The preparation of these compounds begins with commercially available 3-nitroaniline **235** (Scheme 18). Amide formation with either 2-methoxy or 3-chlorobenzoyl chloride was accomplished under standard conditions to afford **236** and **237**, respectively. The reduction of the nitro group via Raney nickel hydrogenation gave anilines **238** and **239**. A parallel synthesis, library approach was used in reactions with acid chlorides and with the aid of resin bound scavengers to provide final compounds **240–255** (Table 17). The hit compound in this series was dibenzamide **240**, which was confirmed to bind at the MPEP binding site

through studies with [^{3}H]-mPEPy ($mGlu_5$ K_i = 1100 nM). Multiple examples were prepared with a methoxy group at R^1 and substituted phenyl rings at R^2. Tolerance for substitution in these cases was limited to the 3-position (compare **241** and **242** to **240**). Other substituents at the 3-position failed to yield compounds with superior potency to hit **240** (**243–246**). Installation of non-benzamide groups at R^2 led to multiple inactive compounds such as benzyl amide **247**. Choosing to hold the 3-chlorobenzamide constant led to a second library of compounds without improvement on hit **240**. Still, several moderately potent compounds were obtained with small cycloalkyl amides (**252** and **253**). Potency quickly fell off if the cycloalkyl amide was too large as noted with cyclopentyl amide **251**. Also of note were isonicotinamide **254** (EC_{50} = 1870 nM; Glu_{max} = 49%) and nicotinamide **255** (EC_{50} = 5540 nM; Glu_{max} = 56%), which acted as PAMs. Such an example is particularly interesting as it constitutes an example of pharmacology mode switching in a non-alkyne $mGlu_5$ series.

Follow up work to the HTS screen yielded a fourth publication in 2010 focused on developing SAR around an oxadiazole hit compound **256** (Table 18).[106] The oxadiazole series was previously disclosed as $mGlu_5$ NAMs in a patent application from NPS Pharmaceuticals;[107] however, Vanderbilt continued work in this series with the goal of developing a new, useful tool compound in a series without an alkyne or amide moiety. Compounds in this series can be prepared in a single step through a condensation reaction of 2-pyridylamidoxime with substituted benzoic acids. Although most new analogues (**257–259**) failed to achieve improved potency relative to hit compound **256**, 3-cyano-5-fluorophenyl analogue **260** was a notable improvement and was selected for extensive evaluation as a potential tool compound. Radioligand binding studies revealed that **260** was fully competitive with [^{3}H]-mPEPy ($mGlu_5$ K_i = 17 nM), suggesting an interaction with the known allosteric binding site. Further studies with the neutral ligand 5MPEP[108] confirmed this interaction. Compound **260** also demonstrated an ability to induce rightward shifts of the glutamate concentration response curve while decreasing the maximal response to glutamate, a profile consistent with noncompetitive inhibition. Compound **260** was determined to be selective over other mGlus. Evaluation of **260** in a modified version of the Geller-Seifter conflict paradigm model[12,82] in rats revealed that the compound dose dependently increases punished responding relative to vehicle at 3 and 10 mg/kg (IP dosing) and significantly decreased unpunished responding a the 10 mg/kg dose. Compound **260** was also efficacious in the mouse marble burying model of anxiety,[77] demonstrating a significant decrease in marble burying relative to vehicle at the 10 mg/kg dose (IP dosing). The anxiolytic effects observed here with **260** were comparable to MTEP, which was run as a positive control. A particularly interesting experiment presented here examined **260** and MTEP in a PCP-induced hyperlocomotion model in rats, a model of psychotomimetic-like activity. Both compounds were dosed IP at 10 mg/kg and while MTEP produced a robust potentiation of PCP induced hyperlocomotion, no such activity was observed with **260**.

In addition to pursuing new $mGlu_5$ NAM scaffolds based on their HTS results, Vanderbilt has also been investigating rational design approaches. One such effort was published recently and described SAR in a series of 3-cyano-5-fluoro-*N*-arylbenzamides.[109] Recognizing the prevalence of 3-cyano-5-fluorophenyl rings found across known $mGlu_5$ NAM scaffolds (see **138**, **203**, **210**, and **260** for examples), chemists used a library approach to rapidly generate new amide analogues prepared from 3-cyano-5-fluorobenzoic acid according to standard methods (Table 19). Several heteroaryl amides were prepared and most new analogues were only weak antagonists as was observed with compound **262**. The 6-methylpyridine analogue **138** was previously described by NIDA (Table 9) and demonstrated the expected potent activity. Isosteric 4-methylthiazole analogue **261** had not been previously described and was equally potent. Tolerance for substitution of the thiazole was limited as exemplified by compound **263**. Noting the weak antagonist activity observed with simple aniline analogue **264**, a series of substituted aniline analogues were prepared.

Anilines substituted with small 3-substituents (**265** and **266**) demonstrated substantially enhanced potency relative to **264**. Also of interest were the results with regioisomeric analogues **267** and **268**. Although their IC_{50} values were nearly identical, like most of the potent compounds reported here, **267** was a full antagonist; however, **268** was a clear partial antagonist. In the case of partial antagonists the complete response curves plateaus whereas full antagonists bring the curve near to zero. In this case, at a 30 μM top concentration of **268**, the amplitude of response as a percentage of maximal response (100 μM glutamate) plateaus at 43%. Radioligand binding studies with [^{3}H]-mPEPy verified the interaction of four compounds (**138**, **261**, **265**, and **266**) with the known allosteric binding site. Following evaluation of the same four compounds in microsomal stability assays, both **261** and **265**, were evaluated in rat pharmacokinetic studies using IP dosing at 10 mg/kg doses. The CNS penetration was quite good with both compounds (brain to plasma ratios = 4.1 (**261**) and 1.4 (**265**)). Furthermore, protein binding studies with each compound (rat plasma = 92.4% bound (**261**) and 93.7% bound (**265**)) indicated that ample free fraction is available to make both potentially interesting tool compounds. Current efforts are focused in that area.

Conclusion

Considering the aforementioned cases of positive clinical reports with mGlu5 NAMs and the immense effort from groups across the globe directed toward the discovery and optimization of many diverse chemotypes, the likelihood of a molecule making it to market in the future would seem high. Extensive effort has identified a number of templates that contain the alkyne moiety found in earlier compounds such as MTEP and MPEP. Other than the previously discovered compound fenobam, current clinical compounds where structures (or generic structures) are in the public domain also contain this functionality. Whether the newer chemotypes described here offer advantages to the alkyne containing compounds remains to be determined. Of particular note is that despite the diversity of chemical scaffolds that have been disclosed, where reported, the interaction of these compounds appears to be with the known allosteric (MPEP) binding site. The discovery of a second allosteric binding site and compounds that interact with it would be a notable advancement and would no doubt spur further research. In any case, the current excitement for this target and approach to new therapeutics should continue to result in new and interesting discoveries for several years to come. Hopefully, such discoveries will also soon translate into useful therapeutics for patients.

Acknowledgments

The author thanks NIDA (RO1 DA023947) and Seaside Therapeutics (VUMC33842) for their support of our programs at the Vanderbilt Center for Neuroscience Drug Discovery focused on the development of negative allosteric modulators of mGlu$_5$.

Abbreviations

7TM	seven transmembrane
Ac	acetyl
ALT	alanine transaminase
Ar	aryl
AUC	area under the curve
BINAP	2,2'-bis(diphenylphosphino)-1,1'-binaphthyl

BOP	Benzotriazole-1-yl-oxy-tris-(dimethylamino)-phosphonium hexafluorophosphate
CDI	carbonyldiimidazole
CHO	Chinese hamster ovary
CNS	central nervous system
dba	dibenzylideneacetone
DCC	*N*,*N*′-dicyclohexylcarbodiimide
DIEA	*N*,*N*-diisopropylethylamine
DMAP	4-dimethylaminopyridine
DME	dimethoxyethane
DMF	*N*,*N*-dimethylformamide
DMSO	dimethylsulfoxide
dppf	1,1'- bis(diphenylphosphanyl) ferrocene
EDC	1-ethyl-3-(3-dimethylaminopropyl) carbodiimide
Et	ethyl
FPS	fear-potentiated startle test
FXS	fragile × syndrome
GERD	gastroesophageal reflux disease
GPCR	G-protein-coupled receptors
HATU	2-(1*H*-7-Azabenzotriazol-1-yl)-1,1,3,3-tetramethyl uronium hexafluorophosphate methanaminium
HEK	human embryonic kidney
HOBt	hydroxybenzotriazole
HPLC	high performance liquid chromatography
HTS	high throughput screening
^{i}Bu	isobutyl
IP	intraperitoneal
^{i}Pr	isopropyl
LELP	lipophilic ligand efficiency metrics
Me	methyl
mGlu	metabotropic glutamate receptor
M-MPEP	2-((3-methoxyphenyl)ethynyl)-6-methylpyridine
MPEP	2-methyl-6-(phenylethynyl) pyridine
mPEPy	3-methoxy-5-(pyridin-2-ylethynyl)pyridine
Ms	methanesulfonyl
MTEP	3-[(2-methyl-1,3-thiazol-4-yl)ethynyl]pyridine

NAM	negative allosteric modulator
NIDA	National Institute on Drug Abuse
^{n}Bu	*n*-butyl
^{n}Pr	*n*-propyl
PAM	positive allosteric modulator
PCP	phencyclidine
PD	Parkinson's disease
PD-LID	Parkinson's disease levodopa-induced dyskinesia
Ph	phenyl
PI	phosphatidylinositol
PKC	protein kinase C
PPA	polyphosphoric acid
PS	polystyrene
pyBOP	(Benzotriazol-1-yloxy)tripyrrolidinophosphonium hexafluorophosphate
SAR	structure activity relationship
SIH	stress-induced hyperthermia
SILE	size independent ligand efficiency
S_NAr	nucleophilic aromatic substitution
^{t}Bu	*tert*-butyl
THF	tetrahydrofuran
Ts	*para*-toluenesulfonic acid
XANTPHOS	4,5-Bis(diphenylphosphino)-9,9-dimethylxanthene

References

1. Schoepp DD, Jane DE, Monn JA. Pharmacological agents acting at subtypes of metabotropic glutamate receptors. Neuropharmacology. 1999; 38:1431–1476. [PubMed: 10530808]
2. Conn PJ, Pin J-P. Pharmacology and functions of metabotropic glutamate receptors. Annu. Rev. Pharmacol. Toxicol. 1997; 37:205–237. [PubMed: 9131252]
3. Knöpfel T, Kuhn R, Allgeier H. Metabotropic glutamate receptors: Novel targets for drug development. J. Med. Chem. 1995; 38:1417–1426. [PubMed: 7738999]
4. Niswender CM, Jones CK, Conn PJ. New therapeutic frontiers for metabotropic glutamate receptors. Curr. Top. Med. Chem. 2005; 5:847–857. [PubMed: 16178730]
5. Ritzén A, Mathiesen JM, Thomsen C. Molecular pharmacology and therapeutic prospects of metabotropic glutamate receptor allosteric modulators. Basic Clin. Pharmacol. Toxicol. 2005; 97:202–213. [PubMed: 16176554]
6. Kew JNC. Positive and negative allosteric modulation of metabotropic glutamate receptors: emerging therapeutic potential. Pharmacol. Ther. 2004; 104:233–244. [PubMed: 15556676]
7. Gasparini F, Lingenhöhl K, Stoehr N, Flor PJ, Heinrich M, Vranesic I, Biollaz M, Allgeier H, Heckendorn R, Urwyler S, Varney MA, Johnson EC, Hess SD, Rao SP, Sacaan AI, Santori EM, Veliocelebi G, Kuhn R. Methyl-6-(phenylethynyl)-pyridine (MPEP), a potent, selective and systematically active mGlu5 receptor antagonist. Neuropharmacology. 1999; 38:1493–1503. [PubMed: 10530811]

8. Cosford ND, Tehrani L, Roppe J, Schweiger E, Smith ND, Anderson J, Bristow L, Brodkin J, Jiang X, McDonald I, Rao S, Washburn M, Varney MA. 3-[(2-Methyl-1,3-thiazol-4-yl)ethynyl]-pyridine: a potent and highly selective metabotropic glutamate subtype 5 receptor antagonist with anxiolytic activity. J. Med. Chem. 2003; 46:204–206. [PubMed: 12519057]

9. Zhu CZ, Wilson SG, Mikusa JP, Wismer CT, Gauvin DM, Lynch JJ, Wade CL, Decker MW, Honore P. Assessing the role of metabotropic glutamate receptor 5 in multiple nociceptive modalities. Eur. J. Pharmacol. 2004; 506:107–118. [PubMed: 15588730]

10. Nicolas LB, Kolb Y, Prinssen EPM. A combined marble burying-locomoter activity test in mice: A practical screening test with sensitivity to different classes of anxiolytics and antidepressants. Eur. J. Pharmacol. 2006; 547:106–115. [PubMed: 16934246]

11. Pietraszek M, Sukhanov I, Maciejak P, Szyndler J, Gravius A, Wislowska A, Plaznik A, Bespalov AY, Danysz W. Anxiolytic-like effects of mGlu1 and mGlu5 receptor antagonists in rats. Eur. J. Pharmacol. 2005; 514:25–34. [PubMed: 15878321]

12. Busse CS, Brodkin J, Tattersall D, Anderson JJ, Warren N, Tehrani L, Bristow LJ, Varney MA, Cosford NDP. The behavioral profile of the potent and selective mGlu5 receptor antagonist 3-(2-methyl-1,3-thiazol-4-yl)ethynyl]pyridine (MTEP) in rodent models of anxiety. Neuropsychopharmacology. 2004; 29:1971–1979. [PubMed: 15305166]

13. Klodzinska A, Tatarczynska E, Chojnacka-Wójcik E, Nowak G, Cosford NDP, Pilc A. Anxiolytic-like effects of MTEP, a potent and selective mGlu5 receptor agonist does not involve GABAA signaling. Neuropharmacology. 2004; 47:342–350. [PubMed: 15275823]

14. Spooren WPJM, Vassout A, Neijt HC, Kuhn R, Gasparini F, Roux S, Porsolt RD, Gentsch C. Anxiolytic-like effects of the prototypical metabotropic glutamate receptor 5 antagonist 2-methyl-6-(phenylethynyl)pyridine in rodents. J. Pharmacol. Exp. Ther. 2000; 295:1267–1275. [PubMed: 11082464]

15. Jensen J, Lehmann A, Uvebrant A, Carlsson A, Jerndal G, Nilsson K, Frisby C, Blackshaw LA, Mattsson JP. Transient lower esophageal sphincter relaxations in dogs are inhibited by a metabotropic glutamate receptor 5 antagonist. Eur. J. Pharmacol. 2005; 519:154–157. [PubMed: 16102747]

16. Frisby CL, Mattsson JP, Jensen JM, Lehmann A, Dent J, Blackshaw LA. Inhibition of transient lower esophageal sphincter relaxation and gastroesophageal reflux by metabotropic glutamate receptor ligands. Gastroenterology. 2005; 129:995–1004. [PubMed: 16143137]

17. de Vrij FMS, Levenga J, van der Linde HC, Koekkoek SK, De Zeeuw CI, Nelson DL, Oostra BA, Willemsen R. Rescue of behavioral phenotype and neuronal protrusion morphology in *Fmr1* KO mice. Neurobiol. Dis. 2008; 31:127–132. [PubMed: 18571098]

18. Yan QJ, Rammal M, Tranfaglia M, Bauchwitz RP. Suppression of two major Fragile × Syndrome mouse model phenotypes by the mGluR5 antagonist MPEP. Neuropharmacology. 2005; 49:1053–1066. [PubMed: 16054174]

19. McGeehan AJ, Olive MF. The mGluR5 antagonist MPEP reduces the conditioned rewarding effects of cocaine but not other drugs of abuse. Synapse. 2003; 47:240–242. [PubMed: 12494407]

20. Chiamulera C, Epping-Jordan MP, Zocchi A, Marcon C, Cottiny C, Tacconi S, Corsi M, Orzi F, Conquet F. Reinforcing and locomotor stimulant effects of cocaine are absent in mGluR5 null mutant mice. Nat. Neurosci. 2001; 4:873–874. [PubMed: 11528416]

21. Martin-Fardon R, Baptista MAS, Dayas CV, Weiss F. Dissociation of the effects of MTEP [3-[(2-Methyl-1,3-thiazol-4-yl)ethynyl]piperidine] on conditioned reinstatement and reinforcement: Comparison between cocaine and a conventional reinforcer. J. Pharmacol. Exp. Ther. 2009; 329:1084–1090. [PubMed: 19258516]

22. Kumaresan V, Yuan M, Yee J, Famous KR, Anderson SM, Schmidt HD, Pierce RC. Metabotropic glutamate receptor 5 (mGluR5) antagonists attenuate cocaine priming- and cue-induced reinstatement of cocaine seeking. Behav. Brain Res. 2009; 202:238–244. [PubMed: 19463707]

23. Bäckstrom P, Hyytiä P. Ionotropic and metabotropic glutamate receptor antagonism attenuates cue-induced cocaine seeking. Neuropsychopharmacology. 2006; 31:778–786. [PubMed: 16123768]

24. Iso Y, Grajkowska E, Wroblewski JT, Davis J, Goeders NE, Johnson KM, Sanker S, Roth BL, Tueckmantel W, Kozikowski AP. Synthesis and structure–activity relationships of 3-[(2-

Methyl-1,3-thiazol-4-yl)ethynyl]pyridine analogues as potent, noncompetitive metabotropic glutamate receptor subtype 5 antagonists; search for cocaine medications. J. Med. Chem. 2006; 49:1080–1100. [PubMed: 16451073]

25. Kenny PJ, Boutrel B, Gasparini F, Koob GF, Markou A. Metabotropic glutamate 5 receptor blockade may attenuate cocaine self-administration by decreasing brain reward function in rats. Psychopharmacology. 2005; 179:247–254. [PubMed: 15602687]
26. Tessari M, Pilla M, Andreoli M, Hutcheson DM, Heidbreder CA. Antagonism at metabotropic glutamate 5 receptors inhibits nicotine- and cocaine-taking behaviours and prevents nicotine-triggered relapse to nicotine-seeking. Eur. J. Pharmacol. 2004; 499:121–133. [PubMed: 15363959]
27. Platt DM, Rowlett JK, Spealman RD. Attenuation of cocaine self-administration in squirrel monkeys following repeated administration of the mGluR5 antagonist MPEP: comparison with dizocilpine. Psychopharmacology. 2008; 200:167–176. [PubMed: 18509621]
28. Lee B, Platt DM, Rowlett JK, Adewale AS, Spealman RD. Attenuation of behavioral effects of cocaine by the metabotropic glutamate receptor 5 antagonist 2-methyl-6-(phenylethynyl)-pyridine in squirrel monkeys: Comparison with dizocilpine. J. Pharmacol. Exp. Ther. 2005; 312:1232–1240. [PubMed: 15550570]
29. Tronci V, Vronskaya S, Montgomery N, Mura D, Balfour DJK. The effects of the mGluR5 receptor antagonist 6-methyl-2-(phenylethynyl)-pyridine (MPEP) on behavioural responses to nicotine. Psychopharmacology. 2010; 211:33–42. [PubMed: 20422403]
30. Kotlinska J, Bochenski M. Comparison of the effects of mGluR1 and mGluR5 antagonists on the expression of behavioral sensitization to the locomotor effect of morphine and the morphine withdrawal jumping in mice. Eur. J. Pharmacol. 2007; 558:113–118. [PubMed: 17222405]
31. Gass JT, Osborne MPH, Watson NL, Brown JL, Olive MF. mGluR5 antagonism attenuates methamphetamine reinforcement and prevents reinstatement of methamphetamine-seeking behavior in rats. Neuropsychopharmacology. 2009; 34:820–833. [PubMed: 18800068]
32. Adams CL, Short JL, Lawrence AJ. Cue-conditioned alcohol seeking in rats following abstinence: Involvement of metabotropic glutamate 5 receptors. Br. J. Pharmacol. 2010; 159:534–542. [PubMed: 20067474]
33. Besheer J, Grondin JJM, Salling MC, Spanos M, Stevenson RA, Hodge CW. Interoceptive effects of alcohol require mGlu5 receptor activity in the nucleus accumbens. J. Neurosci. 2009; 29:9582–9591. [PubMed: 19641121]
34. Gass JT, Olive MF. Role of protein kinase C epsilon (PKCε) in the reduction of ethanol reinforcement due to mGluR5 antagonism in the nucleus accumbens shell. Psychopharmacology. 2009; 204:587–597. [PubMed: 19225761]
35. Schroeder JP, Spanos M, Stevenson JR, Besheer J, Salling M, Hodge CW. Cue-induced reinstatement of alcohol-seeking behavior is associated with increased $ERK_{1/2}$ phosphorylation in specific limbic brain regions: Blockade by the mGluR5 antagonist MPEP. Neuropharmacology. 2008; 55:546–554. [PubMed: 18619984]
36. Lominac KD, Kapasova Z, Hannun RA, Patterson C, Middaugh LD, Szumlinski KK. Behavioral and neurochemical interactions between group 1 mGluR antagonists and ethanol: Potential insight into their anti-addictive properties. Drug Alcohol Depend. 85:142–156. [PubMed: 16697125]
37. Morin N, Grégoire L, Gomez-Mancilla B, Gasparini F, Di Paolo T. Effect of the metabotropic glutamate receptor type 5 antagonists MPEP and MTEP in Parkinsonian monkeys. Neuropharmacology. 2010; 58:981–986. [PubMed: 20074579]
38. Lindsley CW, Emmitte KA. Recent progress in the discovery and development of negative allosteric modulators of mGluR5. Curr. Opin. Drug Discov. Dev. 2009; 12:446–457.
39. Gasparini F, Bilbe G, Gomez-Mancilla B, Spooren W. mGluR5 antagonists: Discovery, characterization and drug development. Curr. Opin. Drug Discov. Dev. 2008; 11:655–665.
40. Jaeschke G, Wettstein JG, Nordquist RE, Spooren W. mGluR5 receptor antagonists and their therapeutic potential. Expert Opin. Ther. Patents. 2008; 18:123–142.
41. Rocher, J-P. Metabotropic glutamate receptors: Translation from discovery to clinical trials. New York, NY, February 23, 2010. The New York Academy of Sciences; New York, NY: 2010. Discovery of novel series of selective mGluR5 negative allosteric modulators.

42. Keywood C, Wakefield M, Tack J. A proof-of-concept study evaluating the effect of ADX10059, a metabotropic glutamate receptor-5 negative allosteric modulator, on acid exposure and symptoms in gastroesophageal reflux disease. Gut. 2009; 58:1192–1199. [PubMed: 19460767]
43. Marin JCA, Goadsby PJ. Glutamatergic fine tuning with ADX-10059: A novel therapeutic approach for migraine? Exp. Opin. Invest. Drugs. 2010; 19:555–561.
44. Goadsby, PJ.; Keywood, CG. Investigation of the role of mGluR5 inhibition in migraine: A proof of concept study of ADX10059 in acute treatment of migraine. 61st annual meeting of the American Academy of Neurology; Seattle, WA. Saint Paul, MN: American Academy of Neurology; 2009. Abstract P06.006
45. Pecknold JC, McClure DJ, Appeltauer L, Wrzesinski L, Allan T. Treatment of anxiety using fenobam (a nonbenzodiazepine) in a double-blind standard (diazepam) placebo-controlled study. J. Clin. Psychopharmacology. 1982; 2:129–132.
46. Berry-Kravis EM, Hessl D, Coffey S, Hervey C, Schneider A, Yuhas J, Hutchinson J, Snape M, Tranfaglia M, Nguyen DV, Hagerman R. A pilot open label, single dose trial of fenobam in adults with fragile × syndrome. J. Med. Genet. 2009; 46:266–271. [PubMed: 19126569]
47. Gasparini, F. mGluR5 antagonists as potential symptomatic therapy for Fragile X Disorder. 239th ACS national meeting; San Francisco, CA. Washingtion, DC: American Chemical Society; 2009. Abstract MEDI 12031
48. Berg, D.; Godau, J.; Trenkwalder, C.; Eggert, K.; Csoti, I.; Storch, A.; Gasparini, F.; Hariry, S.; Johns, D.; Gomez-Mancilla, B. A randomized, controlled trial evaluating AFQ056 in reducing levodopa-induced dyskinesia in patients with Parkinson's disease. 13th International Congress of Parkinson's Disease and Movement Disorders; Paris, France. Milwaukee, WI: The Movement Disorder Society; 2009. Abstract LB-05
49. Addex Pharmaceuticals: Addex' ADX10059 has potential for Parkinson's disease levodopa induced dyskinesia (PD-LID). Press Release. September 14.2009
50. Addex Pharmaceuticals: Addex ADX48621 positive primate Parkinson's data. Press Release. November 24.2009
51. Addex Pharmaceuticals: Development of ADX10059 ended for long-term use. Press Release. December 15.2009
52. Harris G. Promise seen in drug for retardation syndrome. New York Times. April 30.2010 :A1.
53. AstraZeneca PLC: AstraZeneca Development Pipeline. Pipeline Summary. July 30.2009
54. F. Hoffman-LaRoche, Ltd. Roche Pipeline 2010. Pipeline Summary. April 15.2010
55. Seaside Therapeutics: Novel therapies for patients with autism and Fragile × Syndrome. Corporate Fact Sheet. 2010 Quarter 1.
56. Dove P, Granberg K, Isaac M, Någård M, Slassi A. 1,2,4-triazole ether derivatives as modulators of mGluR5. WO 2009/054785 A1. 2009
57. Bratt E, Granberg K, Isaac M, Någård M, Slassi A. Amide linked heteroaromatic derivatives as modulators of mGluR5. WO 2009/054790 A1. 2009
58. Isaac M, Wållberg A. Amino 1,2,4-triazole derivatives as modulators of mGluR5. WO 2009/054794 A1. 2009
59. Wensbo D, Xin T, Stefanac T, Arora J, Edwards L, Isaac M, Slassi A, Stormann TM, McLeod DA, Kers A, Malmberg J, Oscarsson K, Gyback H, Johansson M, Minidis A, Waldman M, Yngve U, Osterwall C. New compounds. WO 2004/014881 A2.
60. Granberg K, Wållberg A. 1,2,4-Triazole aryl *N*-oxides derivatives as modulators of mGluR5. WO 2009/054786 A1. 2009
61. Bratt E, Granberg K. 1,2,3-Triazole pyrrolidine derivatives as modulators of mGluR5. WO 2009/054789 A1. 2009
62. Granberg K, Slassi A, Stefanac T, Wållberg A. 1,2,4-Triazole carboxylic acid derivatives as modulators of mGluR5. WO 2009/054787 A1. 2009
63. Granberg K, Holm B. Aminopyridine derivatives as modulators of mGluR5. WO 2009/054792 A1. 2009
64. Granberg K, Holm B, Någård M. Thiophene 1,2,4-triazole derivatives as modulators of mGluR5. WO 2009/054793 A1. 2009

65. Granberg K, Holm B. Fused pyrrolidine 1,2,4-triazole derivatives as modulators of mGluR5. WO 2009/054791 A1. 2009
66. Hansen TV, Wu P, Fokin VV. One-pot copper(I)-catalyzed synthesis of 3,5-disubstituted isoxazoles. J. Org. Chem. 2005; 70:7761–7764. [PubMed: 16149810]
67. Granberg K, Holm B. Sulphide bridged derivatives as modulators of mGluR5. WO 2010/123451 A1. 2010
68. Corey EJ, Bakshi RK, Shibata S. Highly enantioselective borane reduction of ketones catalyzed by chiral oxazaborolidines. Mechanism and synthetic implications. J. Am. Chem. Soc. 1987; 109:5551–5553.
69. Wágner G, Wéber C, Nyéki O, Nógrádi K, Bielik A, Molnár L, Bobok A, Horvath A, Kiss B, Kolok S, Nagy J, Kurkó D, Gál K, Greiner I, Szombathelyi Z, Keserű GM, Domány G. Hit to lead optimization of disubstituted oxadiazoles and tetrazoles as mGluR5 NAMs. Bioorg. Med. Chem. Lett. 2010; 20:3737–3741. [PubMed: 20483612]
70. Gasparini F, Andres H, Flor PJ, Heinrich M, Inderbitzin W, Lingenhöhl K, Müller H, Munk VC, Omilusik K, Stierlin C, Stoehr N, Vranesic I, Kuhn R. [^{3}H]-M-MPEP, a potent, subtype-selective radioligand for the metabotropic glutamate receptor subtype 5. Bioorg. Med. Chem. Lett. 2002; 12:407–409. [PubMed: 11814808]
71. Nissink JWM. Simple size-independent measure of ligand efficiency. J. Chem. Inf. Model. 2009; 49:1617. [PubMed: 19438171]
72. Keserű GM, Makara GM. The influence of lead discovery strategies on the properties of drug candidates. Nat. Rev. Drug Discov. 2009; 8:203–212. [PubMed: 19247303]
73. Galambos J, Wágner G, Nógrádi K, Bielik A, Molnár L, Bobok A, Horváth A, Kiss B, Kolok S, Nagy J, Kurkó, Bakk ML, Vastag M, Sághy K, Gyertyán I, Gál K, Greiner I, Szombathelyi Z, Keserű GM, Domány G. Carbamoyloximes as novel non-competitive mGlu5 receptor antagonists. Bioorg. Med. Chem. Lett. 2010; 20:4371–4375. [PubMed: 20615697]
74. Vogel JR, Beer B, Clody DE. A simple and reliable conflict procedure for testing anti-anxiety agents. Psychopharmacology. 1971; 21:1–7.
75. Pilla M, Andreoli M, Tessari M, Delle-Fratte S, Roth A, Butler S, Brown F, Shah P, Bettini E, Cavallini P, Benedetti R, Minick D, Smith P, Tehan B, D'Alessandro PD, Lorthioir O, Ball C, Garzya V, Goodacre C, Watson S. The identification of novel orally active mGluR5 antagonist GSK2210875. Bioorg. Med. Chem. Lett. 2010; 20:7521–7524. [PubMed: 21051228]
76. Ferrari L, Crestan V, Sabattini G, Vinco F, Fontana S, Gozzi A. Brain penetration of local anaesthetics in the rat: Implications for experimental neuroscience. J. Neurosci. Methods. 2010; 186:143–149. [PubMed: 19917309]
77. Njung'e K, Handley SL. Evaluation of marble-burying behavior as a model of anxiety. Pharmacol. Biochem. Behav. 1991; 38:63–67. [PubMed: 2017455]
78. Britton TC, Dehlinger V, Fivush AM, Hollinshead SP, Vokits BP. 3-Indazolyl-4-pyridylisothiazoles. WO2009/123855 A1. 2009
79. Dallmann R, Steinlechner S, von Hörsten S, Karl T. Stress-induced hyperthermia in the rat: Comparison of classical and novel recording methods. Lab. Anim. 2006; 40:186–193. [PubMed: 16600078]
80. Jimenez HN, Li G, Doller D, Grenon M, White AD, Guo M, Ma G. Adamantyl diamide derivatives and uses of same. WO 2010/011570 A1. 2010
81. Cosford NDP, Roppe J, Tehrani L, Schweiger EJ, Seiders TJ, Chaudary A, Rao S, Varney MA. [^{3}H]-Methoxymethyl-MTEP and [^{3}H]-methoxy-PEPy: potent and selective radioligands for the metabotropic glutamate subtype 5 (mGlu5) receptor. Bioorg. Med. Chem. Lett. 2003; 13:351. [PubMed: 12565928]
82. Moore NA, Rees G, Sanger G, Tye NC. Effects of olanzapine and other antipsychotic agents on responding maintained by a conflict schedule. Behav. Pharmacol. 1994; 5:196–202. [PubMed: 11224268]
83. Henrich M, Weil T, Müller S, Nagel J, Gravius A, Kauss V, Zemribo R, Erdmane E. Pyrazolopyrimidines, a process for their preparation and their use as medicine. WO 2009/095254 A1. 2009

84. Danysz W, Dekundy A, Hechenberger M, Henrich M, Jatzke C, Nagel J, Parsons CGR, Weil T, Fotins J, Gutcaits A, Kalvinsh I, Zemribo R, Kauss V. Pyrazolopyrimidines, a process for their preparation and the use as a medicine. WO 2008/015271 A1. 2008

85. Kulkarni SS, Newman AH. Design and synthesis of novel heterobiaryl amides as metabotropic glutamate receptor subtype 5 antagonists. Bioorg. Med. Chem. Lett. 2007; 17:2074–2079. [PubMed: 17336520]

86. Kulkarni SS, Nightingale B, Dersch CM, Rothman RB, Newman AH. Design and synthesis of noncompetitive metabotropic glutamate receptor subtype 5 antagonists. Bioorg. Med. Chem. Lett. 2006; 16:3371–3375. [PubMed: 16678408]

87. Kulkarni SS, Zou M-F, Cao J, Deschamps JR, Rodriguez AL, Conn PJ, Newman AH. Structure-activity relationships comparing *N*-(6-methylpyridin-yl)-substituted aryl amides to 2-methyl-6-(substituted-arylethynyl)pyridines or 2-methyl-4-(substituted-arylethynyl)thiazoles as novel metabotrobic glutamate receptor subtype 5 antagonists. J. Med. Chem. 2009; 52:3563–3575. [PubMed: 19445453]

88. Kulkarni SS, Newman AH. Discovery of heterobicyclic templates for novel metabotropic glutamate receptor subtype 5 antagonists. Bioorg. Med. Chem. Lett. 2007; 17:2987–2991. [PubMed: 17446071]

89. Zhang P, Zou M-F, Rodriguez AL, Conn PJ, Newman AH. Structure–activity relationships in a novel series of 7-substituted-aryl quinolines and 5-substituted-aryl benzothiazoles at the metabotropic glutamate receptor subtype 5. Bioorg. Med. Chem. 2010; 18:3026–3035. [PubMed: 20382541]

90. Boice GN, Savarin CG, Murry JA, Conrad K, Matty L, Corley EG, Smitrovich JH, Hughes D. An efficient synthesis of a highly functionalized 4-arylpiperidine. Tetrahedron. 2004; 60:11367–11374.

91. Milbank JBJ, Knauer CS, Augelli-Szafran CE, Sakkab-Tan AT, Lin KK, Yamagata K, Hoffman JK, Zhuang N, Thomas J, Galatsis P, Wendt JA, Mickelson JW, Schwarz RD, Kinsora JJ, Lotarski SM, Stakich K, Gillespie KK, Lam WW, Mutlib AE. Rational design of 7-arylquinolines as non-competitive metabotropic glutamate receptor subtype 5 antagonists. Bioorg. Med. Chem. Lett. 2007; 17:4415–4418. [PubMed: 17590335]

92. Sharma S, Rodriguez AL, Conn PJ, Lindsley CW. Synthesis and SAR of a mGluR5 allosteric partial antagonist lead: Unexpected modulation of pharmacology with slight structural modifications to a 5-(phenylethynyl)pyrimidine scaffold. Bioorg. Med. Chem. Lett. 2008; 18:4098–4101. [PubMed: 18550372]

93. Rodriguez AL, Nong Y, Sekaran NK, Alagille D, Tamagnan GD, Conn PJ. A close structural analog of 2-methyl-6-(phenylethynyl)-pyridine acts as a neutral allosteric site ligand on metabotropic glutamate receptor subtype 5 and blocks the effects of multiple allosteric modulators. Mol. Pharmacol. 2005; 68:1793–1802. [PubMed: 16155210]

94. Spanka C, Glatthar R, Desrayaud S, Fendt M, Orain D, Troxler T, Vranesic I. Piperidyl amides as novel, potent and orally active mGlu5 receptor antagonists with anxiolytic-like activity. Bioorg. Med. Chem. Lett. 2010; 20:184–188. [PubMed: 19931453]

95. Bouwknecht JA, Olivier B, Paylor RE. The stress-induced hyperthermia paradigm as a physiological animal model for anxiety: A review of pharmacological and genetic studies in the mouse. Neurosci. Biobehav. Rev. 2007; 31:41–59. [PubMed: 16618509]

96. Millan MJ, Brocco M. The Vogel conflict test: Procedural aspects, γ-aminobutyric acid, glutamate and monoamines. Eur. J. Pharmacol. 2003; 463:67–96. [PubMed: 12600703]

97. Davis M, Falls WA, Campeau S, Kim M. Fear-potentiated startle: A neural and pharmacological analysis. Behav. Brain Res. 1993; 58:175–198. [PubMed: 8136044]

98. Davis M. Pharmacological and anatomical analysis of fear conditioning using the fear-potentiated startle paradigm. Behav. Neurosci. 1986; 100:814–824. [PubMed: 3545257]

99. Carcache D, Vranesic I, Blanz J, Desrayaud S, Fendt M, Glatthar R. Benzimidazoles as potent and orally active mGlu5 receptor antagonists with an improved PK profile. ACS Med. Chem. Lett. 2011; 2:58–62.

100. Hintermann S, Vranesic I, Allgeier H, Brülisauer A, Hoyer D, Lemaire M, Moenius T, Urwyler S, Whitebread S, Gasparini F, Auberson Y. ABP688, a novel selective and high affinity ligand for

the labeling of mGlu5 receptors: Identification, in vitro pharmacology, pharmacokinetic and biodistribution studies. Bioorg. Med. Chem. 2007; 15:903–914. [PubMed: 17110115]

101. Burdi DF, Hunt R, Fan L, Hu T, Wang J, Guo Z, Huang Z, Wu C, Hardy L, Detheux M, Orsini MA, Quinton MS, Lew R, Spear K. Design, synthesis, and structure-activity relationships of novel bicyclic azole-amines as negative allosteric modulators of metabotropic glutamate receptors. J. Med. Chem. 2010; 53:7107–7118. [PubMed: 20809633]
102. Rodriguez AL, Williams R, Zhou Y, Lindsley SR, Le U, Grier MD, Weaver CD, Conn PJ, Lindsley CW. Discovery and SAR of novel mGluR5 non-competitive antagonists not based on an MPEP chemotype. Bioorg. Med. Chem. Lett. 2009; 19:3209–3213. [PubMed: 19443219]
103. Felts AS, Saleh SA, Le U, Rodriguez AL, Weaver CD, Conn PJ, Lindsley CW, Emmitte KA. Discovery and SAR of 6-substituted-4-anilinoquinazolines as non-competitive antagonists of $mGlu_5$. Bioorg. Med. Chem. Lett. 2009; 19:6623–6626. [PubMed: 19854049]
104. Shipe WD, Wolkenberg SE, Lindsley CW. Accelerating lead development by microwave-enhanced medicinal chemistry. Drug Discov. Today: Technol. 2005; 2:155.
105. Zhou Y, Rodriguez AL, Williams R, Weaver CD, Conn PJ, Lindsley CW. Synthesis and SAR of novel, non-MPEP chemotype mGluR5 NAMs identified by functional HTS. Bioorg. Med. Chem. Lett. 2009; 19:6502–6506. [PubMed: 19875287]
106. Rodriguez AL, Grier MD, Jones CK, Herman EJ, Kane AS, Smith RL, Williams R, Zhou Y, Marlo JE, Days EL, Blatt TN, Jadhav S, Menon UN, Vinson PN, Rook JM, Stauffer SR, Niswender CM, Lindsley CW, Weaver CD, Conn PJ. Discovery of novel allosteric modulators of metabotropic glutamate receptor subtype 5 reveals chemical and functional diversity and in vivo activity in rat behavioral models of anxiolytic and antipsychotic activity. Mol. Pharmacol. 2010; 78:1105–1123. [PubMed: 20923853]
107. Van Wagenen BC, Stormann TM, Moe ST, Sheehan SM, McLeod DA, Smith DL, Isaac MB, Slassi A. Heteropolycyclic compounds and their use as metabotropic glutamate receptor antagonists. 2001
108. Rodriguez AL, Nong Y, Sekaran NK, Alagille D, Tamagnan GD, Conn PJ. A close structural analog of 2-methyl-6-(phenylethynyl)-pyridine acts as a neutral allosteric ligand of metabotropic glutamate receptor subtype 5 and blocks the effects of multiple allosteric modulators. Mol. Pharamacol. 2005; 68:1793–1802.
109. Felts AS, Lindsley SR, Lamb JP, Rodriguez AL, Menon UN, Jadhav S, Jones CK, Conn PJ, Lindsley CW, Emmitte KA. 3-Cyano-5-fluoro-*N*-arylbenzamides as negative allosteric modulators of $mGlu_5$: Identification of easily prepared tool compounds with CNS exposure in rats. Bioorg. Med. Chem. Lett. 2010; 20:4390–4394. [PubMed: 20598884]

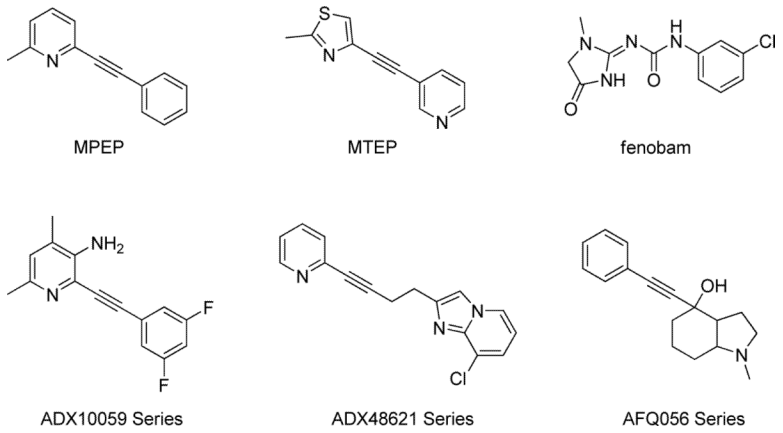

Figure 1.
$mGlu_5$ NAMs MPEP, MTEP, and fenobam. General chemical series of clinical compounds from Addex and Novartis.

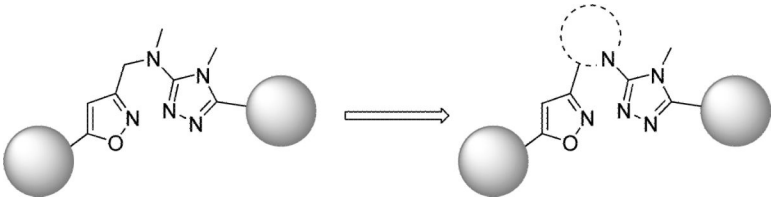

Figure 2.
Constrained analog concept (shown with isoxazole)

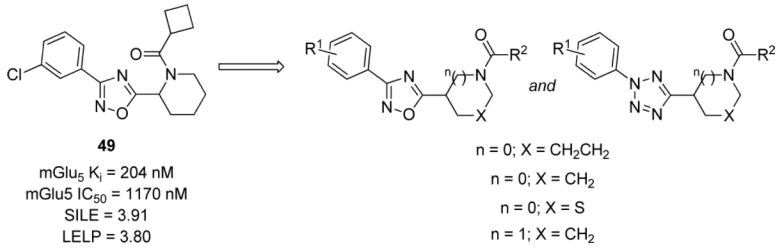

Figure 3.
1,2,4-oxadiazole hit and SAR plan

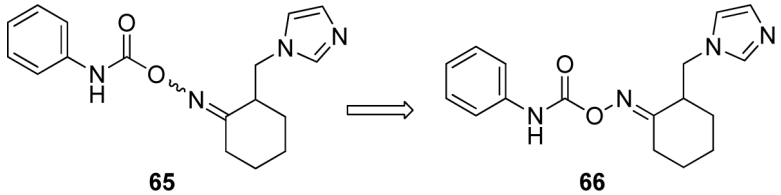

65
$mGlu_5$ K_i = 170 nM
$mGlu_5$ IC_{50} = 273 nM

66
$mGlu_5$ K_i = 104 nM
$mGlu_5$ IC_{50} = 242 nM

Figure 4.
Carbamoyloxime HTS hit and preferred *E*-isomer

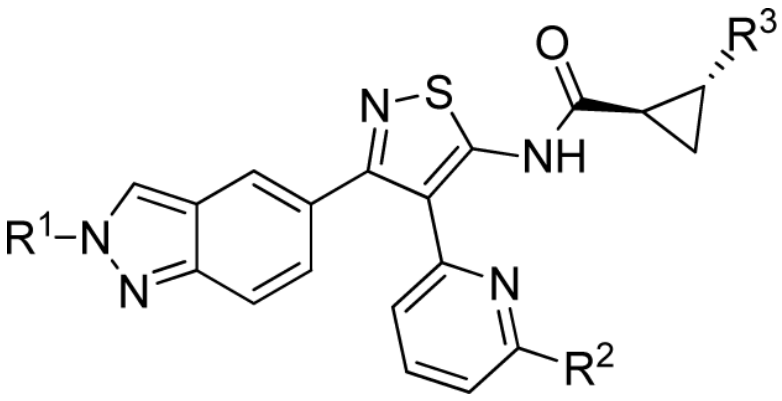

Figure 5.
Isothiazole $mGlu_5$ NAMs

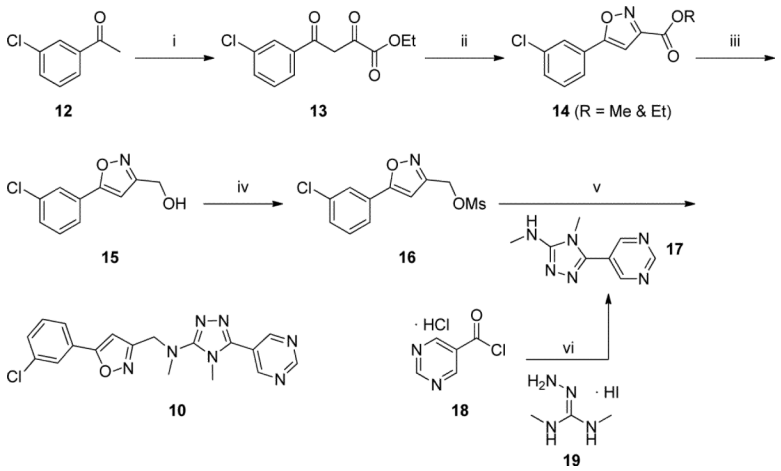

Scheme 1.

[a](i) NaH, DMF, $(EtO_2C)_2$, 0 to 80 °C, *67*% (ii) $NH_2OH{\cdot}HCl$, MeOH, 80 °C, *71*% (iii) $LiAlH_4$, THF, *75*% (iv) NEt_3, MsCl, CH_2Cl_2 (v) NaH, DMF, *79*% (vi) pyridine, −15 to 125 °C, *20*%

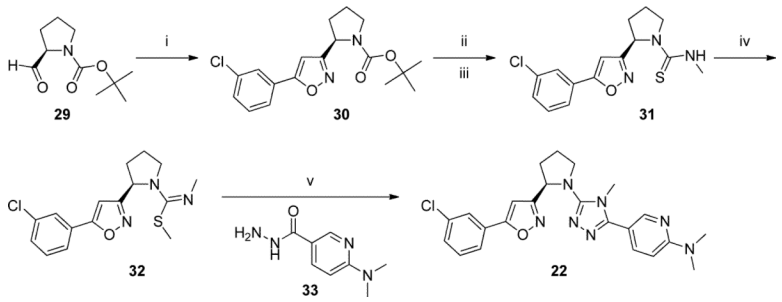

Scheme 2.

[a](i) NaOH, $NH_2OH{\cdot}HCl$, $^tBuOH/H_2O$ (1:1), then $TsN(Cl)Na{\cdot}H_2O$, then $CuSO_4{\cdot}5H_2O$, $NaHCO_3$, 1-chloro-3-ethynylbenzene (ii) F_3CCO_2H, CH_2Cl_2 (iii) MeN=C=S, CH^2Cl_2 (iv) NaO^tBu, THF, MeI (v) ^iPrOH, pyridine, microwave, 150 °C, 2 h., *6*%

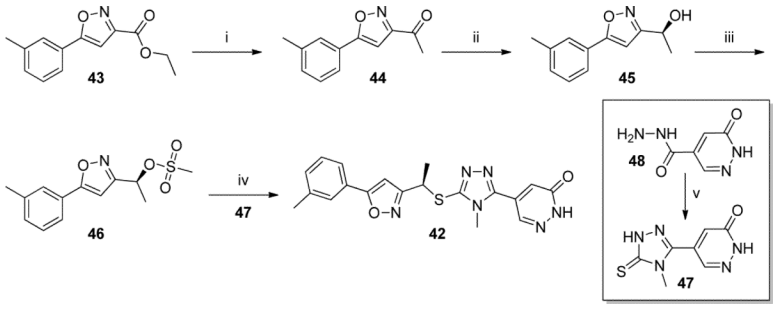

Scheme 3.

[a](i) NEt_3, MeMgBr, PhMe, THF, 0 °C, *46*% (ii) (*R*)-1-methyl-3,3-diphenylhexahydropyrrolo[1,2-c][1,3,2]oxazaborole, $BH_3{\cdot}SMe_2$, PhMe, THF, 0 °C, *84*% (iii) NEt_3, MsCl, CH_2Cl_2 (iv) DIEA, DMSO, 90 °C, *60*% (v) MeN=C=S, H_2O, NaOH, 50 °C

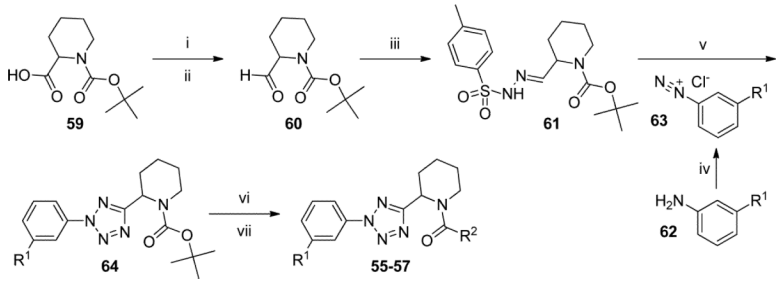

Scheme 4.

[a](i) MeN(OMe)H·HCl, DIEA, DMAP, DCC (ii) $LiAlH_4$, THF, 0 °C, *85*% (2 steps) (iii) $TsNHNH_2$, EtOH, *90*% (iv) $NaNO_2$, HCl, H_2O, 0 °C (v) NaOH, aq. EtOH (vi) HCl, EtOAc, *80–90*% (vii) R^2CO_2H, EDC, NEt_3, CH_2Cl_2

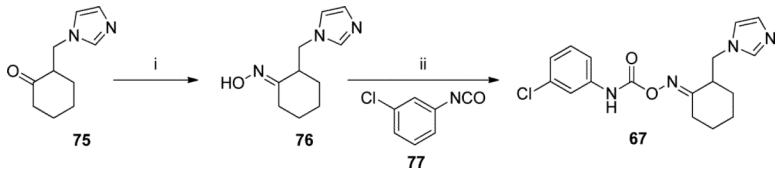

Scheme 5.

[a](i) $NH_2OH{\cdot}HCl$, NaOAc, MeOH, H_2O, 45 °C, then separation of *E* and *Z* isomers, *50–80*%
(ii) CH_2Cl_2, *40–70*%

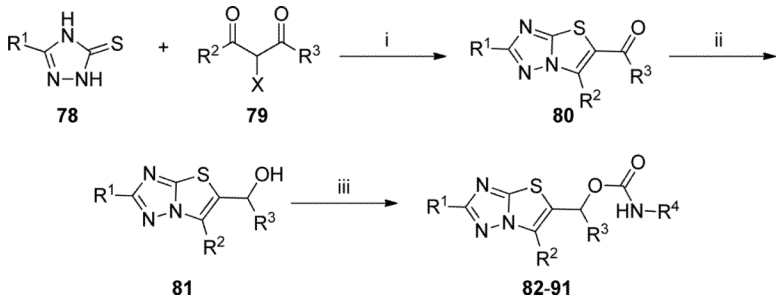

Scheme 6.

[a](i) EtOH, μw, 130 °C, 1 hour (ii) $NaBH_4$ (iii) R^4NCO, μw, 80 °C, 20 minutes or R^4NH_2, CDI, μw, 120 °C, 20 minutes

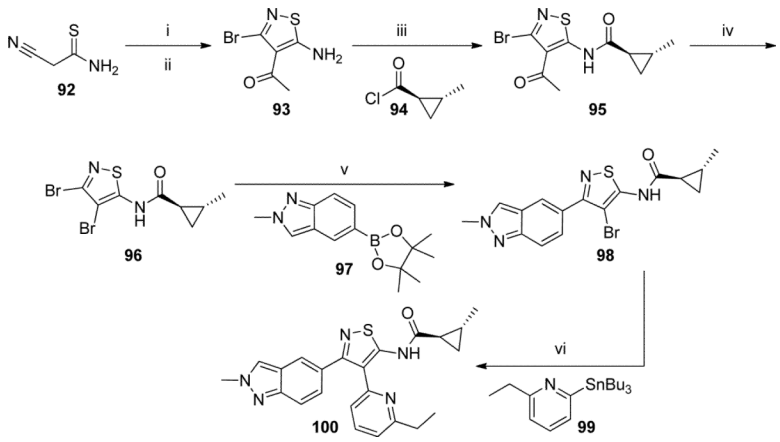

Scheme 7.

[a](i) AcCl, pyridine (ii) Br_2, AcOH, 40 °C, *65%* (2 steps) (iii) NEt_3, CH_2Cl_2, *82%* (iv) aq. NaOH, Br_2, dioxane, 5–10 °C, *85%* (v) 2N aq. Na_2CO_3, DME, $PdCl_2(PPh_3)_2$, 83 °C, *51%* (vi) $PdCl_2(PPh_3)_2$, THF, reflux

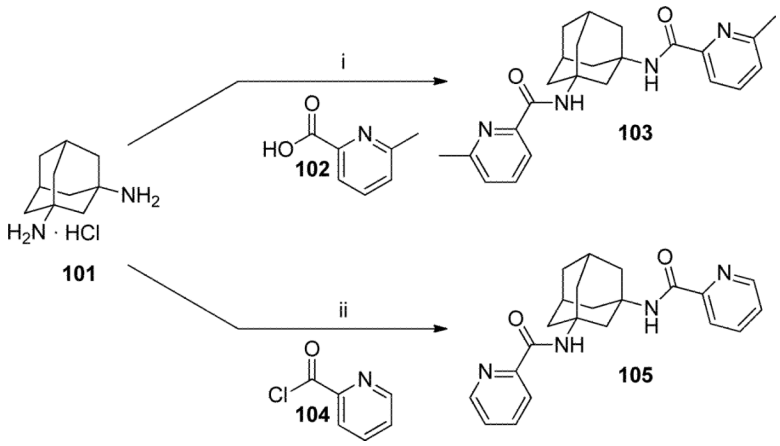

Scheme 8.
[a](i) DIEA, EDC, CH_2Cl_2, *80*% (ii) DIEA, CH_2Cl_2, *50*%

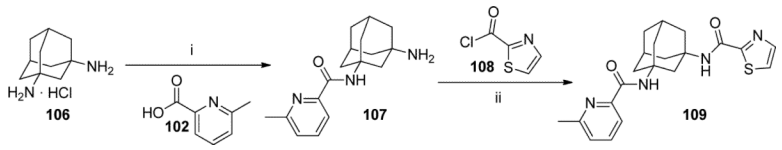

Scheme 9.

[a](i) DIEA, BOP, CH_2Cl_2, *20*% (ii) DIEA, CH_2Cl_2

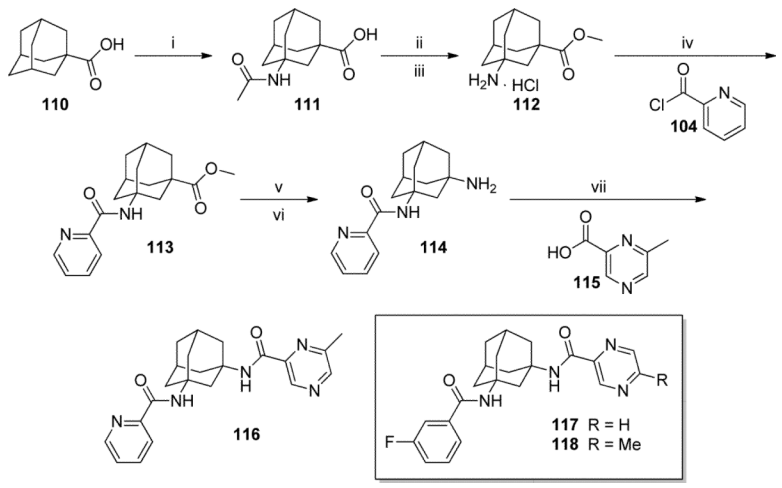

Scheme 10.

[a](i) HNO_3, H_2SO_4, CH_2Cl_2, *74*% (ii) con. HCl, 95 °C (iii) MeOH, $SOCl_2$, 60 °C, *72*% (2 steps) (iv) NEt_3, CH_2Cl_2, *97*% (v) LiOH, H_2O, THF (vi) $(PhO)_2P(O)N_3$, NEt_3, PhMe, 90 °C, *86*% (2 steps) (vii) pyBOP, NEt_3, CH_2Cl_2, *74*%

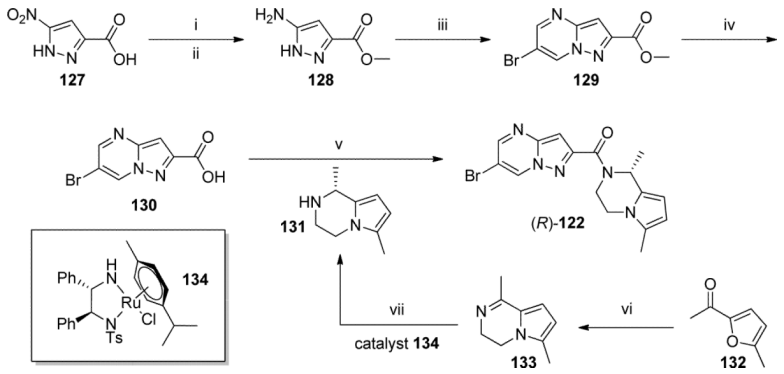

Scheme 11.

[a](i) MeOH, $SOCl_2$, reflux (ii) H_2, Pd/C, THF, AcOH, *88*% (2 steps) (iii) con. HCl, EtOH, $BrCH(CHO)_2$, *18*% (iv) aq. H_2SO_4, heat (v) EDC, HOBt, DMF, 50 °C (vi) $H_2NCH_2CH_2NH_2$, aq. HCl, reflux, *70*% (vii) $Et_3N{\cdot}HCO_2H$, MeCN, *99*%

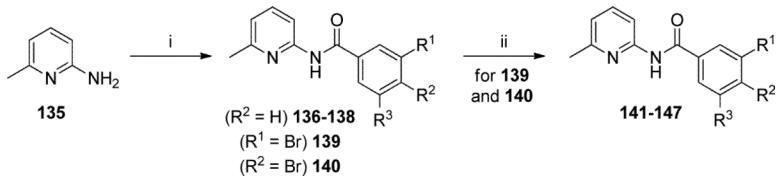

Scheme 12.

[a](i) $ArCO_2H$, CDI, pyridine or ArCOCl, pyridine, NEt_3, CH_2Cl_2, *50–75*% (ii) $ArB(OH)_2$, $Pd(PPh_3)_4$, 2N aq. Na_2CO_3, PhMe, 110 °C or DME/H_2O (3:1), 80 °C, *75–80*%

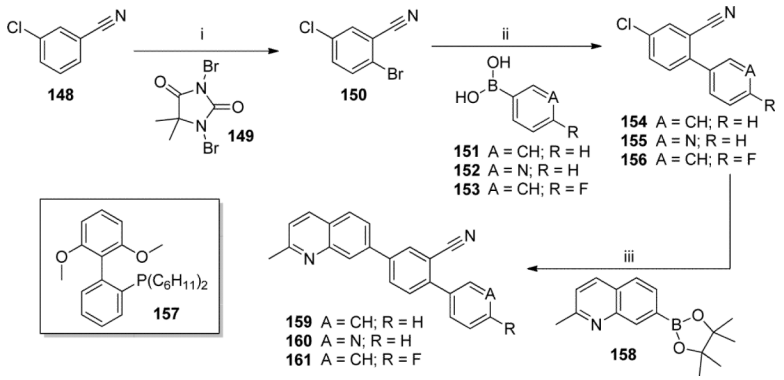

Scheme 13.

[a](i) H_2SO_4, F_3CCO_2H, *76*% (ii) $Pd(PPh_3)_4$, Na_2CO_3, DME, H_2O, 70 °C, *40–75*% (iii) $Pd(OAc)_2$, K_3PO_4, **157**, dioxane, H_2O, 105 °C, *33–42*%

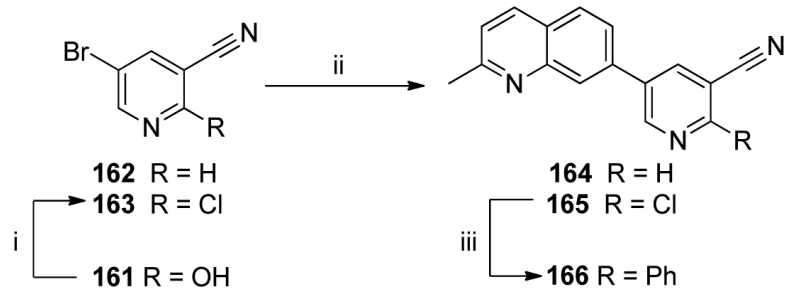

Scheme 14.

[a](i) $POCl_3$, PCl_5, reflux (ii) $PdCl_2$(dppf), Na_2CO_3, **158**, dioxane, H_2O, μw, 140 °C, *65–80*% (iii) $Pd(OAc)_2$, **151**, K_3PO_4, **157**, dioxane, H_2O, μw, 140 °C, *30*%

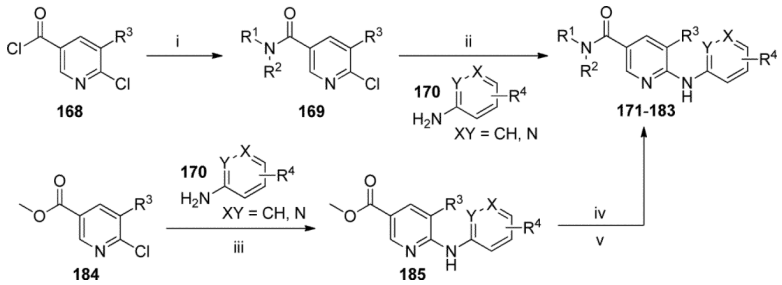

Scheme 15.

[a](i) NEt_3, HNR^1R^2, CH_2Cl_2, 0 °C (ii) AcOH, H_2O (3:7), 95 °C (iii) $Pd(OAc)_2$, BINAP, K_2CO_3, PhMe, 70 °C (iv) 2N aq. NaOH, MeOH, 60 °C (v) HATU, DIEA, DME

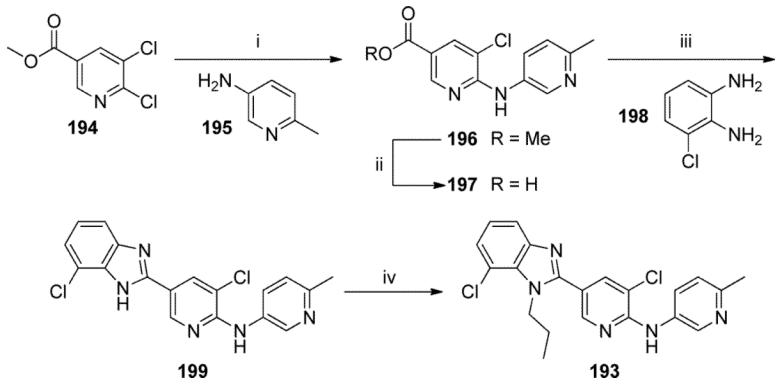

Scheme 16.

[a](i) $Pd_2(dba)_3$, K_2CO_3, BINAP, PhMe, 120 °C, 16 hours, *56*% (ii) 1N aq. NaOH, MeOH, *95*% (iii) PPA, 200 °C, 16 hours, *74*% (iv) NaH, ^{n}PrI, DMF, *10*%

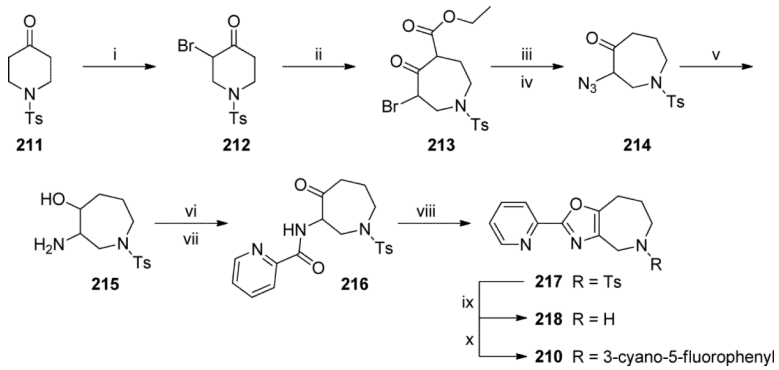

Scheme 17.

[a](i) Br_2, CH_2Cl_2, −5 to −2 °C, *98*% (ii) ethyl diazoacetate, $BF_3{\cdot}OEt_2$, CH_2Cl_2, −5 to 0 °C, *72*% (iii) 3N aq. HCl, dioxane, 100 °C, *90*% (iv) NaN_3, DMF, *80*% (v) $LiAlH_4$, THF, 0 °C, *52*% (vi) picolinic acid, EDC, HOBt, NEt_3, CH_2Cl_2, *80*% (vii) Dess-Martin periodinane, CH_2Cl_2, *92*% (viii) Burgess' reagent, THF, 150 °C, μw, 45 minutes, *78*% (ix) 48% aq. HBr, 100 °C, *74*% (x) 3-bromo-5-fluorobenzonitrile, Pd_2 (dba)$_3$, XANTPHOS, KO^{t}Bu, PhMe, μw, 100 °C, *22*%

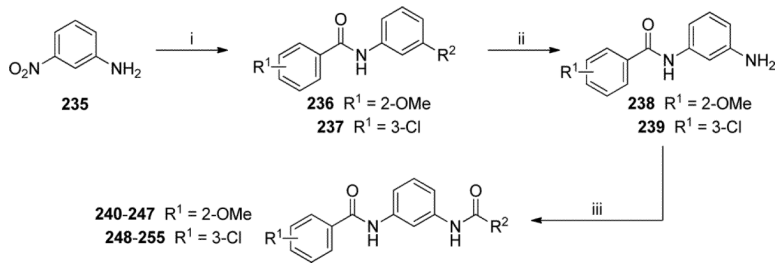

Scheme 18.

[a](i) 2-methoxybenzoyl chloride or 3-chlorobenzoyl chloride, DIEA, DMAP, DMF, *64–89*% (ii) H_2, Raney nickel, EtOH, EtOAc, *89–94*% (iii) R^2COCl, PS-DMAP, PS-DIEA, then PS-isocyanate and PS-trisamine

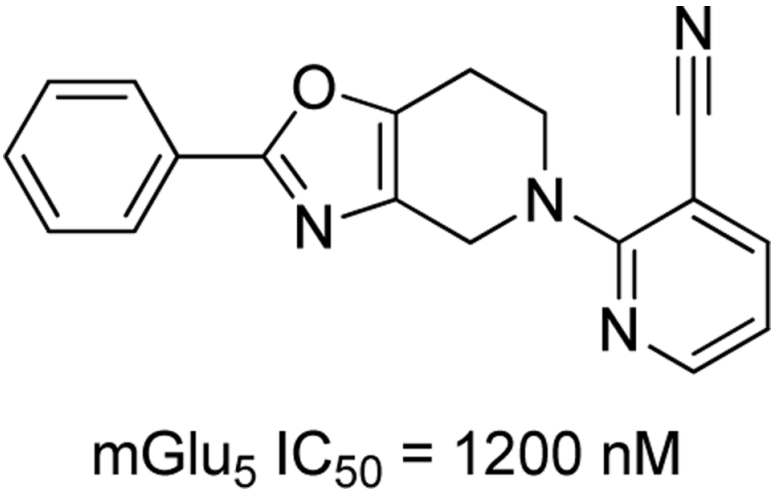

Figure 6.
Hit oxazolopiperidine **200**

Table 1

mGlu$_5$ potency and rat brain penetration SAR in 1,2,4-triazole series

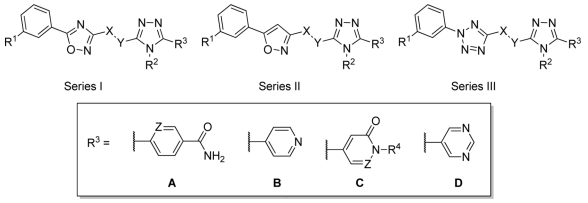

Entry	Series	R^1	X	Y	R^2	R^3	mGlu$_5$ IC_{50} (nM)	Rat B/P Ratio
1	I	Cl	CHMe (*R*)	O	Me	**A** (Z = CH)	8	0.03
2	III	Cl	CHMe (*R*)	O	Me	**A** (Z = CH)	6	0.01
3	III	Cl	CHMe (*R*)	O	Me	**A** (Z = N)	5	0.075
4	II	Cl	C=O	NMe	Me	**B**	37	0.26
5	II	Cl	C=O	NMe	Me	**C** (Z = N; R^4 = H)	62	0.19
6	II	Cl	CH_2	NMe	Et	**C** (Z = N; R^4 = H)	13	<0.01
7	II	Me	CH_2	NEt	Me	**C** (Z = N; R^4 = H)	45	0.01
8	II	Cl	CH_2	NEt	Me	**C** (Z = CH; R^4 = Me)	65	<0.01
9	II	Me	CH_2	NEt	Me	**C** (Z = CH; R^4 = Me)	112	0.22
10	II	Cl	CH_2	NMe	Me	**D**	20	0.16
11	I	Me	CH_2	NEt	Me	**C** (Z = CH; R^4 = Me)	75	<0.01

ACS Chem Neurosci. Author manuscript; available in PMC 2012 August 17.

Table 2

mGlu$_5$ potency and rat brain penetration SAR in constrained cyclic amine 1,2,4-triazole analogues

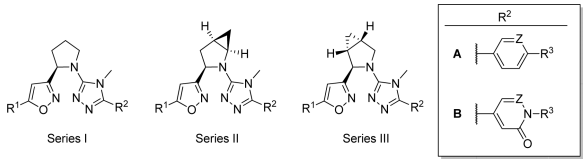

Entry	Series	R^1	R^2	mGlu$_5$ IC_{50} (nM)	Rat B/P Ratio
20	I	3-chlorophenyl	**A** (Z = CH; $R^3 = CO_2NH_2$)	11	< 0.01
21	I	3-chlorophenyl	**A** (Z = N; $R^3 = NH_2$)	< 3	0.085
22	I	3-chlorophenyl	**A** (Z = N; $R^3 = NMe_2$)	39	0.285
23	I	5-chlorothiophen-3-yl	**B** (Z = N; R^3 = H)	39	<0.01
24	II	5-chlorothiophen-3-yl	**B** (Z = N; R^3 = H)	34	0.06
25	I	5-chlorothiophen-3-yl	**B** (Z = N; R^3 = Me)	61	0.16
26	II	3-chlorophenyl	**B** (Z = N; R^3 = H)	32	< 0.01
27	II	3-chlorophenyl	**B** (Z = CH; R^3 = Me)	39	<0.01
28	III	3-chlorophenyl	**B** (Z = N; R^3 = H)	46	not reported

ACS Chem Neurosci. Author manuscript; available in PMC 2012 August 17.

Table 3

mGlu$_5$ potency and rat brain penetration SAR in sulfide bridged analogues

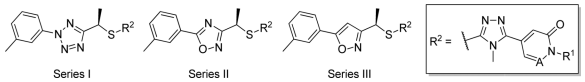

Entry	Series	A	R^1	mGlu$_5$ IC$_{50}$ (nM)	Rat B/P Ratio
34	I	CH	H	19	< 0.01
35	I	CH	Me	87	0.10
36	I	N	H	18	< 0.01
37	II	CH	H	24	0.09
38	II	CH	Me	30	0.16
39	II	N	H	41	0.04
40	III	CH	H	146	< 0.01
41	III	CH	Me	380	0.02
42	III	N	H	19	0.26

Table 4

mGlu$_5$ affinity and potency in the 1,2,4-triazole and tetrazole series

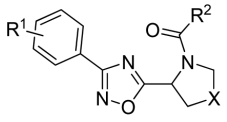

Series I

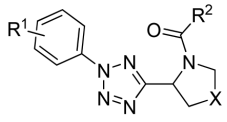

Series II

Entry	Series	R^1	X	R^2	mGlu$_5$ IC_{50} (nM)	mGlu$_5$ K_i (nM)	SILE	LELP
49	I	3-Cl	CH_2CH_2	cyclobutyl	1170	204	3.91	3.80
50	I	3-Me	CH_2CH_2	cyclobutyl	490	126	4.26	3.02
51	I	3-OMe	CH_2CH_2	cyclobutyl	501	182	3.93	3.09
52	I	3-Me	CH_2	-CH_2OMe	30,200	186	4.15	1.77
53	I	3-Cl	CH_2	5-methylthiophen-2-yl	6610	123	3.86	5.05
54	I	3-Cl	S	5-methylthiophen-2-yl	759	83	3.79	5.70
55	II	3-Cl	CH_2CH_2	cyclobutyl	338	78	3.96	3.42
56	II	3-Me	CH_2CH_2	cyclobutyl	224	72	4.17	2.87
57	II	3-Cl	CH_2CH_2	5-bromofuran-2-yl	213	48	3.78	4.31
58	II	3-Cl	CH_2	5-methylthiophen-2-yl	251	89	3.78	4.72

Table 5

$mGlu_5$ affinity and potency in the carbamoyloxime series

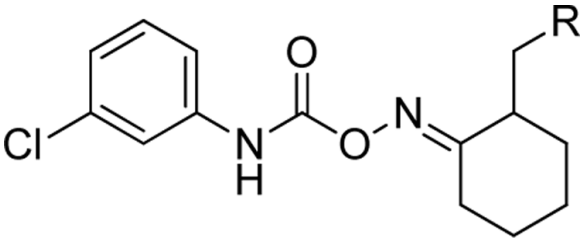

Entry	R	$mGlu_5$ IC_{50} (nM)	$mGlu_5$ K_i (nM)
67	1-imidazolyl	117	11
68	2-thiophenyl	109	9.1
69	3-thiophenyl	477	14
70	4-morpholinyl	—	>1000
71	2-pyridyl	65	40
72	3-pyridyl	15	3
73	phenyl	151	16
74	3-fluorophenyl	127	40

Table 6

mGlu$_5$ potency and protein binding in the thiazolotriazole series

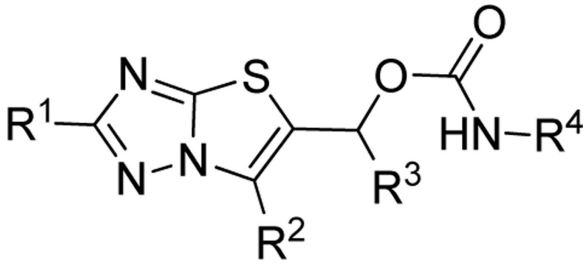

Entry	R^1	R^2	R^3	R^4	mGlu$_5$ IC_{50} (nM)	f_{ub}	pIC_{50} eff
82	H	H	H	phenyl	>30,000	—	—
83	H	Me	H	phenyl	>30,000	—	—
84	H	H	Me	phenyl	10,000	—	—
85	H	Me	Me	phenyl	63	6.8	6.0
86	H	Me	Me	cyclohexyl	3200	—	—
87	H	Me	Me	3-chlorophenyl	40	0.9	5.4
88	H	Me	Me	3-fluorophenyl	50	1.7	5.5
89	H	Me	Me	3-pyridyl	316	28	5.9
90	cyclopropyl	Me	Me	phenyl	13	—	—
91	thiophen-2-yl	Me	Me	phenyl	7.9	<0.1	<5.0

Table 7

Adamantyl diamide efficacy in behavioral assays

Entry	Statistically significant active dose(s) (mg/kg)	
	Mouse marble burying (SC dosing)	Rat conflict test (PO dosing)
103	3, 10, 30	50
105	30	20
109	10, 30	30
116	10, 30	10, 20
117	10. 30	10,30
118	3, 10, 30	20

Table 8

Functional $mGlu_5$ activity and binding affinity in the pyrazolopyrimidine series

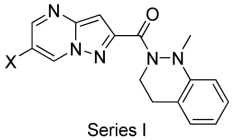

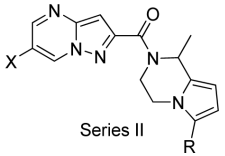

Entry	Series	X	R	Chirality	CHO-K1 $mGlu_5$ IC_{50} (nM)	Astrocytes $mGlu_5$ IC_{50} (nM)	$mGlu_5$ K_i (nM)
119	I	Cl	—	—	166	82	247
120	I	Br	—	—	189	64	281
121	II	Cl	Me	(+/−)	327	87	275
122	II	Br	Me	(+/−)	223	50	219
(*R*)-**122**	II	Br	Me	*R*	118	34	74
123	II	Cl	Cl	(+/−)	91	22	42
124	II	Br	Cl	(+/−)	84	23	45
(*R*)-**124**	II	Br	Cl	*R*	25	7.8	Not Reported
125	II	Cl	Br	(+/−)	34	17	73
126	II	Br	Br	(+/−)	75	15	55

Table 9

Functional $mGlu_5$ activity and binding affinity in the aryl amide series

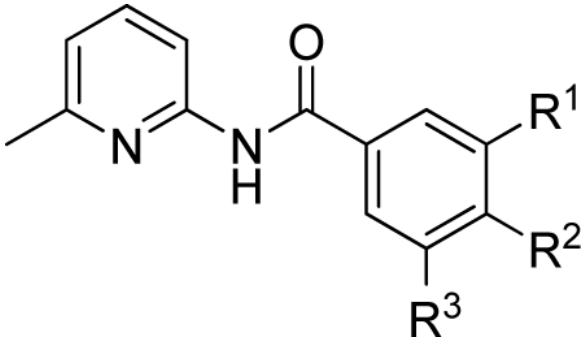

Entry	R^1	R^2	R^3	$mGlu_5$ IC_{50} (nM)	$mGlu_5$ K_i (nM)
136	Cl	H	H	1870	1730
137	CN	H	H	490	330
138	CN	H	F	22	66
141	3-pyridyl	H	F	not tested	702
142	CN	Ph	H	14	9.8
143	H	Ph	H	not tested	7000
144	CN	3-fluorophenyl	H	25	22
145	CN	4-fluorophenyl	H	4.6	134
146	CN	1-naphthyl	H	640	72
147	CN	3-pyridyl	H	>1000	2040

Table 10

Functional mGlu5 activity and binding affinity in the quinoline series

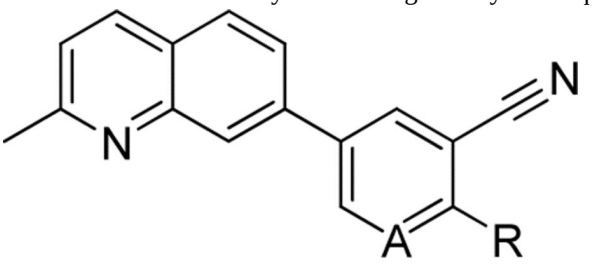

Entry	A	R	$mGlu_5$ IC_{50} (nM)	$mGlu_5$ K_i (nM)
167	CH	H	29	110
151	CH	phenyl	1250	97
152	CH	3-pyridyl	1340	730
153	CH	4-fluorophenyl	692	64
164	N	H	68	100
165	N	Cl	3310	> 10,000
166	N	phenyl	81	97

Table 11

Functional $mGlu_5$ activity in the nicotinamide series

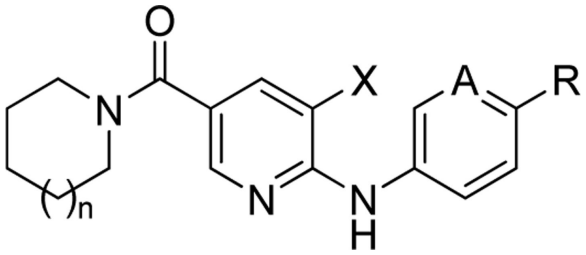

Entry	n	X	A	R	$mGlu_5$ IC_{50} (nM)
171	1	H	CH	Cl	310
172	0	H	CH	Cl	5400
173	2	H	CH	Cl	250
174	3	H	CH	Cl	2300
175	1	H	CH	H	~ 10,000
176	1	H	CH	F	2300
177	1	H	CH	Me	2300
178	1	H	CH	OMe	1800
179	1	H	N	Me	420
180	1	Cl	CH	Cl	95
181	1	Cl	N	Me	87

Table 12

$mGlu_5$ potency, solubility, and intrinsic clearance in the nicotinamide series

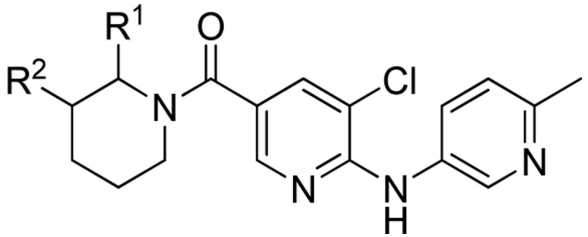

Entry	R^1	R^2	$mGlu_5$ IC_{50} (nM)	Solubility at pH 6.8 (mg/mL)	Rat Cl_{INT} (μL/min/mg)	Human Cl_{INT} (μL/min/mg)
181	H	H	87	150	48	33
(*R*)-**182**	H	*R*-ethyl	40	95	643	322
(*S*)-**182**	H	*S*-ethyl	40	< 3	687	174
(*R*)-**183**	*R*-ethyl	H	32	58	87	89
(*S*)-**183**	*S*-ethyl	H	390	56	190	216

Table 13

mGlu$_5$ potency and intrinsic clearance in 2-benzimidazolyl analogues

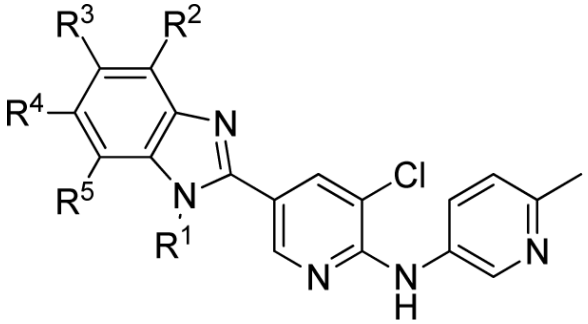

Entry	R^1	R^2	R^3	R^4	R^5	mGlu$_5$ IC$_{50}$ (nM)	Rat Cl$_{INT}$ (μL/min/mg)	Human Cl$_{INT}$ (μL/min/mg)
186	^{n}Pr	H	H	H	H	100	83	158
187	Et	H	H	H	H	110	120	118
188	^{n}Bu	H	H	H	H	360	347	279
189	^{i}Bu	H	H	H	H	110	55	826
190	^{n}Pr	Cl	H	H	H	200	74	69
191	^{n}Pr	H	Cl	H	H	> 500	400	34
192	^{n}Pr	H	H	Cl	H	130	56	33
193	^{n}Pr	H	H	H	Cl	24	83	112

Table 14

mGlu$_5$ potency in tetrahydroazolopyridines and tetrahydroazoloazepines

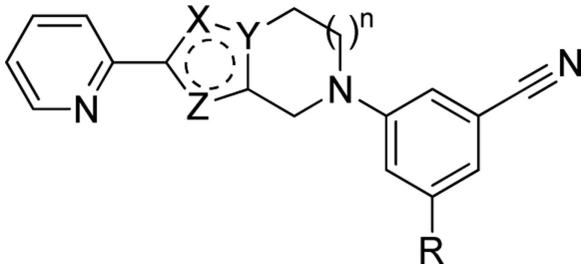

Entry	n	X	Y	z	R	mGlu$_5$ IC$_{50}$ (nM)
201	1	O	C	N	H	60
202	1	N	C	O	H	290
203	1	O	C	N	F	28
204	1	N	C	O	F	54
205	1	N	C	NH	F	34% at 10 μM
206	1	N	C	S	F	52% at 10 μM
207	1	C	N	N	F	153
208	1	N	N	N	F	346
209	2	O	C	N	H	65
210	2	O	C	N	F	16

Table 15

Receptor occupancy and exposures for **203** and **210** in rats

Entry	$mGlu_5$ IC_{50} (nM)	$mGlu_5$ K_i (nM)	% RO	plasma levels (nM)	brain levels (nM)	RO_{50} (mg/kg)
203	28	17	45	2490	1290	> 30
210	16	17	82	1430	1100	0.9

Table 16

$mGlu_5$ potency in the quinazoline series

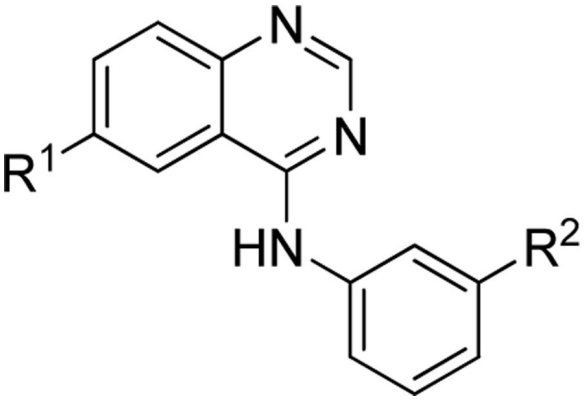

Entry	R^1	R^2	$mGlu_5$ IC_{50} (nM)
219	Br	Cl	256
220	Br	H	>10,000
221	Br	F	1970
222	Br	Br	174
223	Br	Me	246
224	Br	OMe	>10,000
225	Cl	Cl	130
226	F	Cl	311
227	NO_2	Cl	274
228	OMe	Cl	1510
229	Cl	Br	124
230	F	Br	96
231	F	Me	1350
232	F	CF_3	>10,000
233	F	CN	1370
234	F	OMe	>10,000

Table 17

$mGlu_5$ potency in the *N*,*N*'-(1,3-phenylene)diamide series

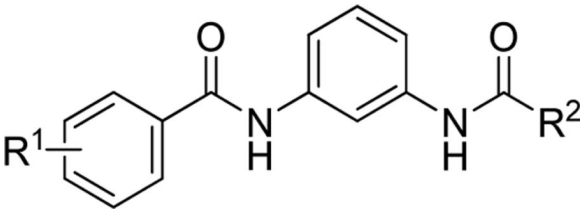

Entry	R^1	R^2	$mGlu_5$ IC_{50} (nM)
240	2-OMe	3-chlorophenyl	880
241	2-OMe	2-chlorophenyl	>30,000
242	2-OMe	4-chlorophenyl	>30,000
243	2-OMe	3-fluorophenyl	6480
244	2-OMe	3-methylphenyl	1350
245	2-OMe	3-(CF_3)phenyl	10,600
246	2-OMe	3-cyanophenyl	1800
247	2-OMe	benzyl	>30,000
248	3-Cl	2-chlorophenyl	2620
249	3-Cl	3-chlorophenyl	>30,000
250	3-C1	2-furyl	4510
251	3-Cl	cyclopentyl	>30,000
252	3-Cl	cyclobutyl	5270
253	3-Cl	cyclopropyl	2230
254	3-Cl	isonicotinamide	PAM
255	3-Cl	nicotinamide	PAM

Table 18

$mGlu_5$ potency in oxadiazole series

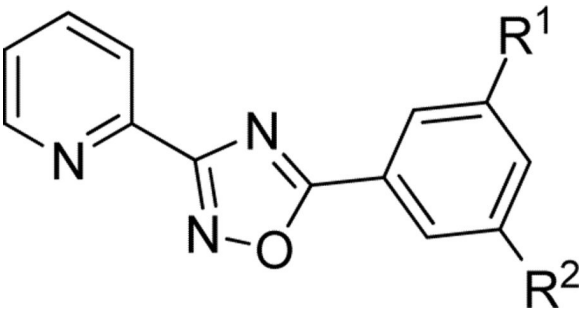

Entry	R^1	R^2	$mGlu_5$ IC_{50} (nM)
256	OMe	OMe	62
257	H	CF_3	2360
258	H	Cl	240
259	H	Br	215
260	F	CN	24

Table 19

$mGlu_5$ potency in 3-cyano-5-fluoro-*N*-arylbenzamide series

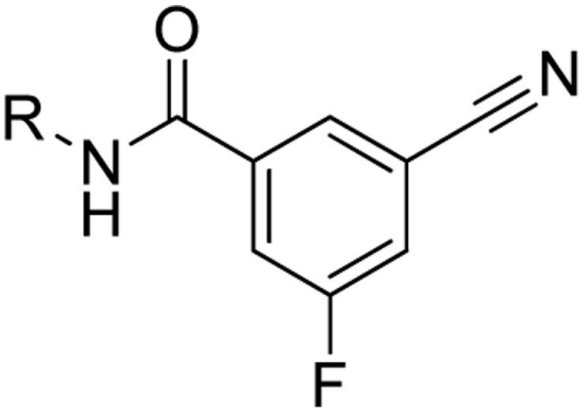

Entry	R	$mGlu_5$ IC_{50} (nM)
138	6-methylpyridin-2-yl	65
261	4-methylthiazol-2-yl	59
262	1-methyl-1*H*-pyrazol-3-yl	>10,000
263	4-cyclopropylthiazol-2-yl	900
264	phenyl	5440
265	3-chlorophenyl	45
266	3-methylphenyl	122
267	3-chloro-2-fluorophenyl	347
268	3-chloro-4-fluorophenyl	377